

DISSERTATION

EFFECT OF BONE GEOMETRY ON STRESS DISTRIBUTION PATTERNS IN THE  
EQUINE METACARPOPHALANGEAL JOINT

Submitted by

Katrina L. Easton

Graduate Degree Program in Bioengineering

In partial fulfillment of the requirements

For the Degree of Doctor of Philosophy

Colorado State University

Fort Collins, Colorado

Spring 2012

Doctoral Committee:

Advisor: Chris Kawcak

Wayne McIlwraith

Christian Puttlitz

Sue James

Kevin Shelburne

Paul Heyliger

Copyright by Katrina L. Easton 2012  
All Rights Reserved

## ABSTRACT

### EFFECT OF BONE GEOMETRY ON STRESS DISTRIBUTION PATTERNS IN THE EQUINE METACARPOPHALANGEAL JOINT

Catastrophic injury of the equine metacarpophalangeal joint is of major concern for both the equine practitioner and the American public. It is one of the major reasons for retirement and sometimes euthanasia of Thoroughbred racehorses. The most common type of catastrophic injury is fracture of the proximal sesamoid bones and lateral condyle of the third metacarpal bone. Many times these injuries are so disastrous that there is no possibility of fixing them. Even in the injuries that are able to be fixed, complications arising from the fracture such as support limb laminitis may ultimately lead to the demise of the horse. Therefore, prevention of these types of injuries is key. In order to decrease the incidence of injury, it is important to understand the risk factors and pathogenesis of disease that leads to them.

This project was established to create a finite element model of the equine metacarpophalangeal joint in order to investigate possible risk factors, namely bone geometry, and its effect on the stress distribution pattern in the joint. The first part of the study involved *in vitro* experiments in order to provide a comprehensive dataset of ligament, tendon, and bone strain and pressure distribution in the joint with which to validate the finite element model. Eight forelimbs from eight different horses were tested on an MTS machine to a load equivalent to that found at the gallop. Beyond providing data for validation, the study was the first to the author's knowledge to measure surface contact pressure between the distal condyles of the third metacarpal bone and the

proximal sesamoid bones. A pressure distribution pattern that could lead to an area of high tension in the area of the parasagittal groove was found. This result could help explain the high incidence of lateral condylar fractures that initiate in this location.

The second part of this study focused on the development and validation of a finite element model of the metacarpophalangeal joint. A model was created based on computed tomography (CT) data. It included the third metacarpal bone, the proximal phalanx, the proximal sesamoid bones, the suspensory ligament, medial and lateral collateral ligaments, medial and lateral collateral sesamoidean ligaments, medial and lateral oblique sesamoidean ligaments, and the straight sesamoidean ligament. The mesh resolution was varied to create three models to allow for convergence. The converged model was then validated using data from the previous part of the study as well as data from the literature. The result was a finite element model containing 121,533 nodes, 112,633 hexahedral elements, and 10 non-linear springs.

The final section of this study used the converged and validated finite element model to study the effect of varying bone geometry. The model was morphed based on CT data from three horses: control, lateral condylar fracture, and contralateral limb to lateral condylar fracture. There was an area similar between all three groups of increased stress in the palmar aspect of the parasagittal grooves where fractures are thought to initiate. Other results showed distinct differences in the stress distribution pattern between the three groups. Further investigation into these differences may help increase the understanding of a horse's predisposition to injury.

In conclusion, this study has shown that joint geometry plays a role in the stress distribution patterns found in the equine metacarpophalangeal joint. The differences in

these patterns between the three groups may help explain the increased risk of a catastrophic injury for some horses. Further studies are warranted to better define the parameters leading to these changes.

## ACKNOWLEDGMENTS

I would like to acknowledge my graduate committee, especially my advisor Dr. Chris Kawcak for allowing me to undertake this research. I would also like to thank Dr. Puttlitz for allowing me to use his computing facilities and for his engineering input, Dr. McIlwraith for his clinical input, Dr. James and Dr. Shelburne for their inputs on the mechanical aspects of the study, and Dr. Heyliger for teaching me about mechanics and finite element modeling through some of the best classes I have ever taken.

This study was funded by several organizations including the Gail Holmes Equine Orthopaedic Research Center, the College Research Council at Colorado State University, the Grayson Jockey Club, and a predoctoral fellowship from the National Institute of Arthritis, Musculoskeletal and Skin Diseases (F31AR056192).

I would also like to thank several individuals that were essential in this study. Matt Petty was essential in his help with the *in vitro* studies and Chelsea Zimmerman for measurement of the parameters on the many CT scans. I would also like to thank Wes Womack and Snehal Shetye for their help with the finite element modeling as well as the other graduate students and staff in Dr. Puttlitz's laboratory. Dr. Tim Parkin should also be acknowledged for providing the majority of the CT scans as well as the MCP joints for the study on geometry.

Most of all, I would like to thank my family, especially my Mama who was always there with support and words of encouragement throughout my seven years in the combined DVM/PhD program.

## TABLE OF CONTENTS

<b>ABSTRACT</b> .....	<b>ii</b>
<b>ACKNOWLEDGEMENTS</b> .....	<b>v</b>
<b>CHAPTER 1: BACKGROUND AND SIGNIFICANCE</b> .....	<b>1</b>
RACEHORSES, INJURY, AND PUBLIC PERCEPTION.....	1
<i>Incidence of injury in racehorses</i> .....	2
RISK FACTORS FOR INJURY .....	4
<i>Age and Gender</i> .....	5
<i>Chronic cyclic fatigue and preexisting pathology</i> .....	5
<i>Conformation and bone geometry</i> .....	7
<i>Neuromuscular control</i> .....	9
<i>Training and race-related factors</i> .....	10
CURRENT THERAPIES.....	12
EARLY DETECTION OF JOINT PROBLEMS.....	14
<i>Prerace screenings</i> .....	14
<i>Diagnostic imaging</i> .....	15
<i>The finite element method</i> .....	16
<i>Failure criteria and bone fracture</i> .....	17
STUDY GOALS AND SIGNIFICANCE.....	19
<i>Significance</i> .....	19
<i>Study goals and hypotheses</i> .....	20
REFERENCES .....	22
<b>CHAPTER 2: EX VIVO BONE, LIGAMENT, AND TENDON STRAIN AND CONTACT PRESSURE IN THE EQUINE METACARPOPHALANGEAL JOINT AT WALK, TROT, AND GALLOP LOADS</b> .....	<b>30</b>
INTRODUCTION.....	30
MATERIALS AND METHODS .....	32
<i>General loading protocol</i> .....	32
<i>Ligament and tendon strain</i> .....	33
<i>Summary of data collection</i> .....	34
<i>Bone strain</i> .....	35
<i>Contact pressure</i> .....	36
<i>Data collection and analysis</i> .....	37
RESULTS.....	39
<i>Ligament and tendon strain</i> .....	40
<i>Bone strain</i> .....	41
<i>Contact pressure</i> .....	42
DISCUSSION .....	44
REFERENCES .....	51

<b>CHAPTER 3: DEVELOPMENT AND VALIDATION OF A THREE DIMENSIONAL FINITE ELEMENT MODEL OF THE EQUINE METACARPOPHALANGEAL JOINT .....</b>	<b>54</b>
INTRODUCTION.....	54
MATERIALS AND METHODS .....	56
<i>Image acquisition and segmentation</i> .....	56
<i>Mesh generation</i> .....	57
<i>Material properties</i> .....	57
<i>Boundary conditions and loading</i> .....	59
<i>Convergence</i> .....	60
<i>Validation</i> .....	60
RESULTS.....	61
<i>Convergence</i> .....	61
<i>Validation</i> .....	62
DISCUSSION .....	66
REFERENCES.....	69
<b>CHAPTER 4: EFFECT OF BONE GEOMETRY ON CONTACT STRESS IN THE EQUINE METACARPOPHALANGEAL JOINT .....</b>	<b>72</b>
INTRODUCTION.....	72
MATERIALS AND METHODS .....	73
<i>Selection of bone geometry data</i> .....	73
<i>Morphing the model</i> .....	74
<i>Boundary conditions and loading</i> .....	74
<i>Analysis</i> .....	74
RESULTS.....	75
DISCUSSION .....	82
REFERENCES.....	87
<b>SUMMARY AND FUTURE DIRECTIONS.....</b>	<b>90</b>

## CHAPTER 1: BACKGROUND AND SIGNIFICANCE

### RACEHORSES, INJURY, AND PUBLIC PERCEPTION

Catastrophic failure of the equine distal limb is the most common cause of euthanasia in Thoroughbred racehorses [1]. It is of major concern to both equine practitioners and the general American public. After the high profile catastrophic injuries of Barbaro and Eight Belles in the 2006 Preakness and 2008 Kentucky Derby respectively, the American public called for reform in the racing industry. A congressional hearing entitled “Breeding, Drugs, and Breakdowns: The State of Thoroughbred Horseracing and the Welfare of the Thoroughbred<sup>a</sup>” was held on June 19, 2008. Experts and long-time affiliates of the racing industry convened to give testimony and their views on the steps needed to be taken to reform the sport and better provide for the welfare of the Thoroughbred racehorse. Many of them discussed:

- The durability of the racehorse and how some people believe that it has declined over the years based on the statistics that show fewer starts per horse and shorter careers now than in 1960;
- Musculoskeletal injury and how its incidence has increased;

---

<sup>a</sup> Committee on Energy and Commerce. “Breeding, Drugs, and Breakdowns: The State of Thoroughbred Horseracing and the Welfare of the Thoroughbred.” 2008. [http://energycommerce.house.gov/index.php?option=com\\_content&view=article&id=1353&catid=27&Itemid=58](http://energycommerce.house.gov/index.php?option=com_content&view=article&id=1353&catid=27&Itemid=58). Accessed 2009 Sept 05.

- Current practices by regulatory veterinarians to attempt to ensure that racehorses at the track are healthy and sound; and
- Ongoing research investigating methods of early diagnosis and improved treatment modalities of bone and joint disease.

Further research in the area of catastrophic injuries is needed in order to improve the welfare of the Thoroughbred racehorse. This research includes determining risk factors for injury, enhanced methods for the detection of subclinical disease, and improved treatment modalities.

#### *Incidence of injury in racehorses*

Overall fatality rate for racehorses due to racing or training ranges from 0.44 to 1 per 1000 starts depending on the geographic location and type of racing [1-4]. Musculoskeletal injuries account for the majority of injuries and fatalities regardless of the geographic location or the type of race: flat, steeple, hurdle, or national hunt flat [2,3,6,7]. In a study on California race tracks, musculoskeletal injuries accounted for 95% and 91% of racing and training related fatal injuries respectively [1]. In addition at California tracks, the proportion of fatalities due to musculoskeletal injuries has gradually increased from 1991-2005 [9].

Most (71-83%) of these musculoskeletal injuries occur in the forelimbs [2,6] and involve the metacarpophalangeal joint (MCP) and/or the suspensory apparatus (Figure 1.1). In a study by McKee [3], it was found that forelimb fractures were responsible for the majority of catastrophic injuries in the United Kingdom. Johnson et al. [7] found that fractures accounted for 84-85% and ruptured ligaments accounted for 10-11% of the

musculoskeletal injuries on California racetracks. At racetracks in California, New Mexico, Texas, and Kentucky, fractures of the proximal sesamoid bones and third metacarpal bone (MC III) were the most common fractures [1,7]. In California, injuries to the suspensory apparatus and MC III were the most common fatal injuries [7].

Results are similar in the United Kingdom. In 2004, Parkin et al. [10] found that lateral condylar fractures of MC III were the most common fractures overall, biaxial proximal sesamoid bone fractures were the most common in all weather flat races, and proximal phalanx fractures were the most common in turf flat races.

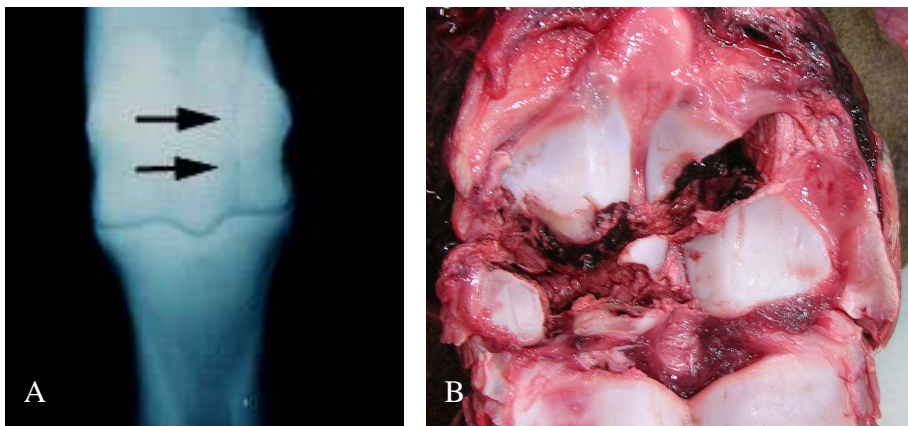


**Figure 1.1:** A) Radiograph of a complete lateral condylar fracture (arrows) and B) photograph of biaxial proximal sesamoid bone fractures.

In a study done in 2006, it was found that in Thoroughbred racehorses in the United Kingdom, the incidence of fatal lateral condylar fractures was 2.4/10,000 starts [11]. Seventy-two percent (54/75) occurred in the forelimbs, 48% in the right forelimb and 24% in the left forelimb. Forty-seven percent of these fractures affected the inside limb, 69% included fractures of the proximal sesamoid bones, and 17% included

fractures of the proximal sesamoid bones combined with fractures of the proximal phalanx.

The distribution of injury between right and left forelimbs varies between studies. Some studies report a significantly greater number of injuries in the left forelimb [1,4] while others do not report any limb differences [7]. Parkin et al. [12] found no significant association between direction of the race and side of the fracture. However, there was a strong association between the most used lead forelimb and the direction of the race and racehorses were 6.3 times more likely to fracture the limb that was leading at the time of fracture.

While the exact statistics differ between tracks and types of racing, one thing remains the same between them all; musculoskeletal injuries, specifically of the MCP and suspensory apparatus, account for the majority of career ending and catastrophic injuries in racehorses.

## RISK FACTORS FOR INJURY

There have been numerous studies investigating possible risk factors for injury during racing and training of racehorses. These factors include horse, training, and race related factors. Some factors such as age, gender, and genetics cannot be controlled, but others such as joint injury and overuse, muscle weakness, and nerve injury can be reduced through proper training, gait modifications, and biomechanical alterations. However, once a joint or supporting structure is injured, adaptations due to the injury may significantly increase the risk for subsequent injury [13-15].

### *Age and Gender*

The effect of age varies by study. Estberg et al. [1] found that 4 year old horses were at a 2 fold greater risk in comparison to 3 year old horses. Other studies have also found that the risk of breakdown increased with the age of the horse [6,13,16,17]. However, another study found no difference between 2 year old horses and horses  $\geq 3$  years old [18].

Some studies have found that geldings [19] and male racehorses in general [1] have a greater risk of injury while other studies have found that gender affects the category of injury; male horses had more catastrophic injuries while females had more career ending injuries [20].

### *Chronic cyclic fatigue and preexisting pathology*

As athletes, horses naturally suffer from repetitive, overuse injuries that can be found in humans as well. These injuries can lead to the long term consequence of osteoarthritis in both species (Figure 1.2). In addition, the overuse injuries and their consequences can progress rapidly in a horse allowing for changes to be seen within a short period of time.

Chronic cyclical loading can lead to abnormal bone adaptation which results in sclerotic or necrotic bone as well as cartilage fibrillation and erosion in the superficial layers [5]. This fatigue damage can weaken the bone such that it is less able to withstand the stress associated with racing or even everyday life. In investigating racehorses with condylar fractures of the third metacarpal/metatarsal bones, racehorses without a condylar fracture, and nonracehorses, Radtke et al. [21] found that the presence of wear

lines, articular cartilage erosions, subchondral bone (SCB) loss, and cracking of the condylar grooves were more severe in racehorses than nonracehorses even though the nonracehorses were older. Parkin et al. [11] also found indications of preexisting pathology in the non-fractured limbs of horses that had sustained lateral condylar fractures of the third metacarpus/metatarsus. Seventy-three percent had some form of macroscopic cartilage pathology with the most common sites being the lateral (63%) and medial (55%) parasagittal grooves. The pathology present included visible fissures and cartilage erosion and discoloration. Other pathologic changes included cartilage erosion along the transverse ridges, full thickness erosion exposing SCB palmar/plantar to the transverse ridges, and linear wear lines parallel to the sagittal ridge.

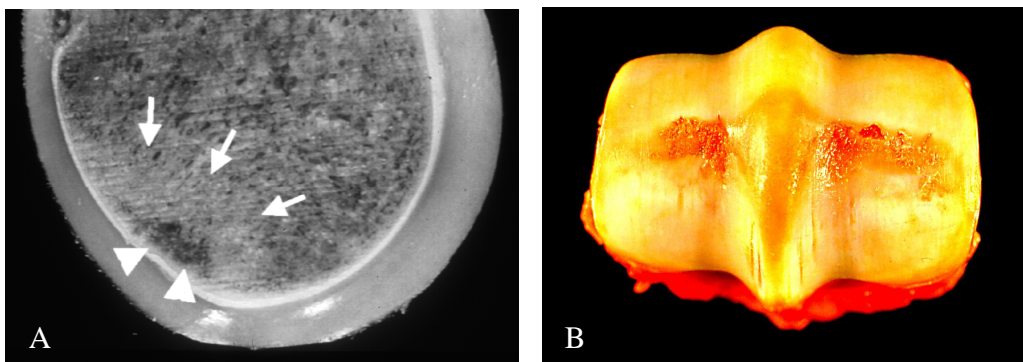


**Figure 1.2:** Examples of osteochondral damage in the equine MCP including A) subchondral bone sclerosis (arrows) and necrosis (arrowheads) [5]; and B) articular cartilage wear lines and erosions typical of osteoarthritic lesions [8].

Studies looking at sites other than the distal condyles of the third metacarpus/metatarsus also show similar results. In one study, the majority (10/13) of the racehorses with a complete humeral fracture had gross evidence of a periosteal callus suggesting the presence of a preexisting stress fracture [22]. Preexisting subclinical to mild suspensory apparatus injury and abnormality of the suspensory ligament found

during prerace physical inspection were found to be positively associated with increased risk of injury [13,17].

This fatigue-related damage also appears to be reflected in the density pattern of subchondral bone in horses and humans [23,24]. The equine MCP has been shown to be a consistent site of overload arthrosis [5]. Riggs et al. [24] found a pattern of SCB sclerosis in the parasagittal groove of the MCP of horses that was associated with linear defects in the overlying mineralized articular cartilage and is a common site for fracture. The authors also found that the areas immediately adjacent and subjacent to the SCB sclerosis had intense focal remodeling. In a study by Nugent et al. [25], the authors found marked site-associated variations in the structure, biochemical, and biomechanical properties of articular cartilage in the equine distal third metacarpal condyle and concluded that not only can these properties of a tissue be influenced by variations in loading within different regions of an articular surface, but that the biomechanical environment can also initiate degenerative changes.

#### *Conformation and bone geometry*

Variations in loading of different regions in a joint and the biomechanical environment can be greatly influenced by how the bones within a joint contact each other and how that contact changes with varying loads. This can depend significantly on whole limb conformation as well as bone geometry. Contact area in the MCP has been found to increase as load increases [26-28]. Brama et al. [28] also found that the dorsal articular margin, an area not normally loaded under low loading conditions such as walking and standing, had the highest peak pressures as the load increased. In addition, fatigue such

as at the end of a race can result in extreme hyperextension in the MCP resulting in stresses on the bones and the cartilage in areas not normally loaded at low load conditions.

Joint geometry and conformational differences such as offset knees and an increase in front pastern length were both found to be risk factors for musculoskeletal problems in the forelimb of the racing Thoroughbred [29]. Hoof shape and balance have also been found to be possible risk factors for catastrophic musculoskeletal injury in Thoroughbred racehorses. Decreased frog to wall distance difference, sole area difference, and toe angle were associated with increased odds of suspensory apparatus failure and fracture of the distal condyle of MC III. Decreased ground surface width difference and increased toe-heel angle were also associated with increased odds of suspensory apparatus failure [30]. Preliminary studies in the laboratory have shown the width of the lateral MC III condyle being small in comparison to the medial MC III condyle is a significant indicator of OA and osteochondral fracture in racehorses (Figure 1.3, [31]).

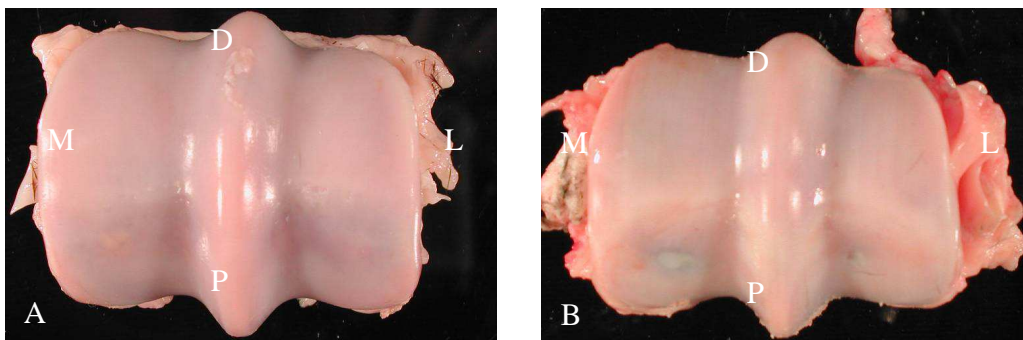


**Figure 1.3:** A) Normal conformation of the distal condyles of MC III. B) The lateral condylar width is small in comparison to the medial condylar width. This has been associated with osteochondral fracture and OA. M = medial, L = lateral, P = palmar, D = dorsal.

Nunamaker et al. [32] found that there were significant differences between the Thoroughbred and the Standardbred racehorse. The Standardbred horse starts out with a smaller minimum moment of inertia in MC III as a yearling than the Thoroughbred horse, but after training the Thoroughbred horse has a greater minimum amount of inertia. The authors hypothesized that this greater modeling and remodeling phase in the young Thoroughbred occurring during racing and training may explain the increased incidence of fractures in comparison to Standardbred racehorses.

#### *Neuromuscular control*

In a study by Santilli et al. [33], the authors investigated muscle activation patterns in human athletes with ankle instability and found that there was a significant decrease in peroneus longus muscle activity on the injured side in comparison to the uninjured side. This suggests that changes in muscle activation patterns may play an important role in joint disease. While these alterations may represent an initial effort by the body to combat pain, muscular weakness, and joint laxity, these adaptations may ultimately speed the progression of disease by altering load magnitude and distribution [34]. This altered loading pattern can lead to maladaptation of bone remodeling [35]. In addition, lack of neuromuscular control can lead to joint laxity and altered biomechanical loading. These alterations may also be one of the initiating factors of disease by contributing to strain, overuse, compensatory movement patterns, and ultimately injury. Sensorimotor training to improve functional stability and postural control in the ankle has been shown to reduce the risk of ankle injury [36,37]. Based on these studies,

understanding neuromuscular control and adaptations due to injury may be important in gaining insight into the factors leading to injury reoccurrence and progression of disease.

#### *Training and race-related factors*

Although no significant association was found in a study by Hill et al. [13], the odds ratio suggested that toe grabs and longer distances at speed may be associated with increased risk of subclinical to mild suspensory apparatus injury. This is important since in the same study it was found that these subclinical to mild injuries were positively associated with increased risk of musculoskeletal injury. Parkin et al. [38] also found that lateral condylar fractures of the third metacarpus/metatarsus were more common in longer races. In contrast, another study found that the shorter the race distance the greater the incidence of injury [17]. The authors of this study hypothesized that this could have been a spurious association, that shorter races may be associated with greater speed which could predispose to injury, or that there may be a number of covariates since in this particular study race distance may be associated with class of race and race number both of which were associated with increased odds for injury.

Racehorses with reduced exercise during the last 30 or 60 days preceding injury, horses doing no gallop work during training and horses in their first year of racing were at a significantly increased risk of sustaining a musculoskeletal injury [19,38]. In addition, an extended interval since the last race was only marginally not significant [19]. A study by Cohen et al. [20] did find a significant association with injury to the superficial digital flexor tendon (SDFT) and an interval of greater than 60 days between the race in which the horse was injured and the previous race.

Cohen et al. [20] found that the odds ratios for toe grabs were 1.63 - 2.93 depending on toe grab height suggesting a possible association with increased risk of musculoskeletal injury. However, similar to the study by Hill et al. [13], toe grab height was not found to have a significant effect (all of the confidence intervals included 1.0). In a study on California racetracks, front shoe toe grabs were found to be a potential risk factor for fatal musculoskeletal injury, suspensory apparatus failure, and fracture of the distal condyle of MC III. Odds increased with higher toe grabs, i.e. no toe grabs to low to regular toe grabs [39].

On Kentucky, Texas, and New Mexico tracks, it was found that racetrack, class of race, and race number  $< 6$  (races earlier in the day) were all significantly associated with injury. On New York racetracks, it was also found that horses raced in the later races (race number  $\geq 4$ ) were at a decreased risk [16]. In addition during the race, stumbling, physical interaction, change in lead limb during the 12 seconds preceding injury, finishing in the back half, and being in the front half of the pack during the stretch were significant factors in injured racehorses [17,18,20].

In summary, there are many factors that may contribute to injury on race day. These factors include race related factors such as track surface, type of race, length of race, and class of race. Horse related factors ranging from shoes to training regimen also play an important role.

## CURRENT THERAPIES

Fractures of the bones of the MCP can be repaired although prognosis varies depending on location and severity of the fracture. Treatment can range from rest to invasive surgery for the attachment of fracture fixation devices. Rest can be an effective treatment especially for non-displaced, incomplete fractures. In a clinical report of 5 horses with incomplete fracture of the distal palmar aspect of MC III, 4 of the 5 horses returned to racing at their previous levels after rest and a gradual return to exercise [40]. It was concluded that conservative treatment carried a good prognosis, but early recognition of these fractures before displacement was important.

Arthroscopy is another important method for treatment of MCP injuries. It is the treatment of choice for osteochondral chip fractures of the proximo-medial/lateral eminence of the proximal phalanx and is done to decrease synovitis and prevent further degenerative joint disease [41,42]. In a study investigating this type of fracture in 336 horses, 92% of the Thoroughbred racehorses with only fragments returned to racing (71% at the same or higher level) compared to only 74% of those that had fragments plus other fetlock lesions (53% at the same or higher level; [43]). Again as with non-displaced, incomplete fractures, early recognition and treatment was felt to be important for a good prognosis for return to work at the previous level.

Fracture fixation devices are commonly used for fractures that need to be stabilized. Horses with non-displaced fractures, although they can heal with conservative treatment, may require less convalescent time with lag screw fixation of the fracture [44]. For proximal sesamoid bone fractures that are less than one-third of the bone,

arthroscopic removal is the preferred choice of treatment. However, internal fixation such as lag screw fixation or circumferential wiring is recommended for larger fractures especially those in the basilar or midbody region as these are more likely to develop degenerative joint disease and restricted range of motion with only conservative treatment [42].

Bone grafts and substitutes can be used to enhance fracture healing. The most common type is autogenous cancellous bone from the sternum, tuber coxae, or the proximal tibia. Hydroxyapatite has been used experimentally in the horse with mixed results [45]. Tricalcium phosphate, both by itself and impregnated with gentamicin, has also been used experimentally to enhance bone healing [46,47].

In severe cases such as bilateral proximal sesamoid fractures and extremely comminuted fractures, arthrodesis may be the only option other than euthanasia due to the enormous amount of soft tissue damage and vascular supply disruption that can lead to significant degenerative joint disease. Arthrodesis can provide a good prognosis for return to pain free unrestricted movement. However, it needs to be done in a timely fashion. Prognosis decreases when it is chosen as a last resort to failed conservative treatment or when evidence of laminitis is already present in the opposing foot [48].

Although the fracture in some cases can be mechanically fixed and the initial injury may be healing fine, complications related to the fracture may ultimately lead to the euthanasia of the horse. One of the major goals of the therapies described is to return the injured limb to weight bearing as quickly as possible in order to minimize the chance of development of support limb laminitis. In cases of severe laminitis leading to unmanageable pain, the horse should be humanely euthanized [49]. Early recognition and

treatment of injuries is important in maximizing the probability of a good prognosis for repair and minimizing degenerative changes and pain.

## EARLY DETECTION OF JOINT PROBLEMS

### *Prerace screenings*

Prerace physical inspections are an important first step in ensuring that horses are healthy and sound enough to race on race day. Regulatory veterinarians assess each horse before the race, during the race, and after the race. They have the authority to require a horse be withdrawn from competing if it is determined to be injured or otherwise unsound. “This protocol is comparable to an individual being accompanied through each work day by a risk assessment advisor and emergency care physician.”<sup>b</sup>

Horses that were assessed to be at increased risk of injury by regulatory veterinarians had odds of musculoskeletal injury, injury of the suspensory apparatus, and injury of the SDFT 5.5 to 13.5 times greater than those not assessed to be at increased risk [18,20]. In addition, horses where an abnormality of the SDFT was found during prerace inspection were significantly more likely to be injured [13,17]. In one study however, of the 81 injured horses, only 5 (6.3%) had an assessment of increased risk [18]. In another study, only 1.6% of the high risk race starts resulted in injury [17]. So even given the significant association between prerace physical inspections and odds of musculoskeletal injury, prerace physical inspections lack sufficient sensitivity and

---

<sup>b</sup> Committee on Energy and Commerce. “Breeding, Drugs, and Breakdowns: The State of Thoroughbred Horseracing and the Welfare of the Thoroughbred.” Testimony of Dr. Mary C. Scollay. 2008. [http://energycommerce.house.gov/cmte\\_mtgs/110-ctcp-hrg.061908.Horseracing.shtml](http://energycommerce.house.gov/cmte_mtgs/110-ctcp-hrg.061908.Horseracing.shtml). Accessed 2008 Sept 05.

specificity to be the sole means of identifying horses that will sustain injury and excluding racehorses from competition. Other factors need to be identified.

Biomarkers for bone turnover also represent a possible prerace method for assessing horses. It is possible to distinguish changes in biomarkers due to disease from the changes due to exercise [50]. In one study, sequential blood samples were taken on racing Thoroughbreds in Southern California.<sup>c</sup> Changes in biomarkers could be seen 6 weeks prior to an injury occurring. Accuracy was 70%. However, combining blood biomarkers with physical inspections could increase the sensitivity and specificity of determining horses at risk. If major risk is determined to the point of precluding a horse from racing, diagnostic imaging could then be performed to determine the area of preexisting damage or injury.

#### *Diagnostic imaging*

Nuclear scintigraphy can be useful in the detection of stress fractures in the humerus, radius, tibia, and third metacarpal bones [40,51,52]. Using computed tomography (CT) and/or magnetic resonance imaging (MRI) also provides a method of tracking pathologic changes in joint tissues as well as measuring a patient's response to treatment. Computed tomography is especially useful in the evaluation of bone and can detect osteolysis and osteogenesis, subchondral bone erosions and subtle internal and external osseous remodeling and reactions before conventional radiography [53]. In addition, it can be used to investigate the long term stresses acting on a joint *in vivo* [54]

---

<sup>c</sup> Committee on Energy and Commerce. "Breeding, Drugs, and Breakdowns: The State of Thoroughbred Horseracing and the Welfare of the Thoroughbred." Testimony of Dr. Wayne McIlwraith. 2008. [http://energycommerce.house.gov/cmte\\_mtgs/110-ctcp-hrg.061908.Horseracing.shtml](http://energycommerce.house.gov/cmte_mtgs/110-ctcp-hrg.061908.Horseracing.shtml). Accessed 2008 Sept 05.

and provide reasonable estimates of elastic modulus, yield stress, ultimate stress, ash density, and strain energy density at yield and at ultimate failure [55]. While MRI can be used to image osseous structures, it can also provide high resolution detail of soft tissue structures as well. A number of studies have used MRI to investigate joint contact area [56-58]. Cartilage volume and thickness as well as quantitative measurements of cartilage composition and bone structure can also be determined using MRI [59-61]. Magnetic resonance images have also been used for the creation of 3D finite element models with an accurate representation of complex muscle architectures and geometries [62]. These models can be used to estimate the stresses and strains within a joint as well as muscle moment arms *in vivo* [63-65].

#### *The finite element method*

Finite element (FE) modeling based on CT and/or MRI data represents a non-invasive *in vivo* method of determining contact and stress patterns within a joint. Anderson et al. [66] found good agreement between results from a CT based FE model and experimentally measured contact pressure distribution values and contact area in the human ankle. Finite element models represent a unique way of taking patient specific geometries and determining stresses and strains unique to a specific geometry without destructive mechanical testing. Various studies have investigated trabecular bone failure in bovine tibia specimens [67], femoral fracture load in humans [68], human vertebral bone compressive strength [69], stress and strain in the canine proximal femur [70], and prediction of stress fractures in the human tibia and equine MC III [71]. All of these studies were in agreement, that FE modeling provided a powerful tool to accurately

investigate various patient specific parameters. Finite element models can assist in predicting bone strength and fracture risk without destructive testing allowing it to be used *in vivo* on a patient specific basis.

Finite element models can also assist in elucidating pathogenesis of posttraumatic degenerative disease. It was found that fractured human ankles had higher peak contact stress exposure and greater area with high exposure than contralateral intact ankles [72,73]. Incongruity and deep sockets in an idealized model of the humeroulnar joint predicted high tensile stresses as the joint socket was spread apart during loading [74]. The model predicted subchondral bone density patterns consistent with what was determined experimentally. The authors concluded that subchondral bone density may not be a direct measure of the adjacent articular pressure in incongruous joints with deep sockets. This finding reiterates the importance of bone geometry in the stresses experienced within a joint.

The use of finite element modeling represents an excellent method of investigating biological systems non-destructively. In addition, it can provide predictions for *in vivo* parameters that could not be measured otherwise.

#### *Failure criteria and bone fracture*

Many studies have investigated failure criteria and their application to bone fracture. The prevalent criteria are generally classified into one of two broad categories: stress based or strain based. Maximum principal stress, maximum shear stress (Tresca), maximum strain energy of distortion (Hencky-von Mises or von Mises), and Drucker-Prager (modified von Mises) are four of the widely used stress based failure criteria.

Within the strain based category, maximum principal strain and maximum shear strain are commonly used.

Despite the many studies, there is currently no gold standard (i.e. no general agreement as to which criteria to use). Some studies advocate a strain based theory. In a finite element study, Schileo et al. [75] compared maximum principal strain, maximum principal stress, and von Mises stress to experimental load to failure results. The authors found that the load at failure was close to experimental results for the maximum principal strain failure criteria whereas both stress based failure criteria underestimated the load at failure, i.e. failure was predicted at a lower load than what was experimentally determined. However, another study showed that the yield load as predicted by the strain based criteria was lower than that predicted by the stress based criteria [76].

Other studies have promoted stress based failure criteria theories. Keyak et al. [77] compared nine different theories across two femoral loading conditions, single limb stance and fall impact. While all the theories showed a significant correlation with experimental results, the authors argued that two of the stress based failure criteria, von Mises and Tresca, were the most robust.

Although there are limitations to all of the failure criteria mentioned, they all combine the individual components of a multiaxial stress state into an equivalent uniaxial stress [78]. This is a benefit over comparing each individual stress or strain component to some yield or fracture load. For the purposes of the current study, the von Mises stress was chosen. The von Mises theory uses the concept of strain energy of distortion. The theory is that only the stress that leads to distortion or shape change will cause failure [78]. The theory has been used for such things as to predict femoral fracture load [79],

investigate the biomechanics of burst fractures [80], and examine fracture fixation [81] to name a few, all with good success.

## STUDY GOALS AND SIGNIFICANCE

### *Significance*

Joint disease in horses is naturally occurring, rapidly progressive, and is a major concern to equine practitioners especially those that work with equine athletes. It is not uncommon to see advanced disease in 3-5 year old horses due to repetitive use. The MCP of racehorses is especially susceptible to a wide variety of injuries as described above. Musculoskeletal conditions are also one of the leading causes of disability among humans in the United States. For example, osteoarthritis (OA) alone affects an estimated 21 million adults [82] and can result in work and leisure activity limitations and even feelings of helplessness, anxiety, or depression [83].

In both humans and horses, OA is characterized by articular cartilage degeneration with variable amounts of subchondral bone sclerosis and remodeling [84-87]. Because of the loss in mechanical and material properties, the articular cartilage and SCB have decreased load absorption and distribution capabilities predisposing them to further damage.

The years 2002-2011 were declared the Bone and Joint Decade in the United States of America. It was part of a worldwide initiative, which began in the year 2000, aimed at increasing the awareness of musculoskeletal diseases, advancing the understanding and treatment of the various conditions, and improving quality of life. The

cause of OA is not known; however, joint injury and overuse are risk factors which may predispose a person or an animal to OA later in life. While treatment and physical therapy modalities are improving, once OA begins it is a progressive, degenerative disease that may ultimately result in complete loss of function. The best treatment is prevention. This is especially true in the case of horses where lack of prevention of musculoskeletal injuries can mean euthanasia.

However, with all of the possible variations in loading parameters such as magnitude, rate, and repetitiveness, combined with patient conformation, gait patterns, loading history, and neuromuscular variations, the study of causative factors of fracture and injury is difficult at best. The use of computer models provides a method of investigating individual variables separately and in conjunction by allowing the user to change parameters such as bone geometry, joint laxity, and material properties. In this way, parameters that show promise of having major effects on prevention or predisposition to injury and disease can be determined thus narrowing the possibilities without having to sacrifice large numbers of animals for controlled experimental studies. In addition, it can assist in determining what information is important to record in prospective studies.

#### *Study goals and hypotheses*

At present, prerace physical inspections are not sensitive nor specific enough to be used as the sole criteria for racehorses to be excluded from racing even though there is an association between odds of musculoskeletal injury and assessment of increased risk [17,18,20]. Additional measures need to be determined.

The objective of this study focused on determining how the stress distribution within the metacarpophalangeal joint, the most commonly injured joint in racehorses, changed with different bone geometries and if certain geometries such as asymmetric condyles of the distal third metacarpus and degree of condylar flattening predisposed the racehorse to musculoskeletal injury. The overarching goal of this project was to provide additional measures for veterinarians to use to assess the risk of injury and prevent career ending and catastrophic fractures of the MCP in racehorses.

The central hypothesis of this study was that the stress distribution in and around the joint would differ due to variations in joint geometry and that these stress patterns would dictate, at least in part, the predisposition of an individual to injury. This hypothesis was investigated through the completion of two specific aims:

1. Development and validation of a 3D finite element model of the equine MCP
2. Application of the finite element model to investigate the stress distribution pattern in the joint and how this pattern changed due to variations in bone geometry

The results of the current study in conjunction with prerace physical inspections and fluid biomarkers can lead to enhanced screening for the prevention of musculoskeletal injuries in racehorses. In a broader context, the methods developed provide a valuable technique for investigating joint disease and can lead to insight into the pathogenesis of OA and other osteochondral diseases as well as possible methods of ultimately preventing the disease from ever initiating or injury from ever occurring.

## REFERENCES

- [1] Estberg L, Stover SM, Gardner IA, Johnson BJ, Case JT, Ardans A, Read DH, Anderson ML, Barr BC, Daft BM, Kinde H, Moore J, Stoltz J, Woods LW. Fatal musculoskeletal injuries incurred during racing and training in Thoroughbreds. *J Am Vet Med Assoc* 1996;208:92-96.
- [2] Boden LA, Anderson GA, Charles JA, Morgan KL, Morton JM, Parkin TD, Slocombe RF, Clarke AF. Risk of fatality and causes of death of Thoroughbred horses associated with racing in Victoria, Australia: 1989-2004. *Equine Vet J* 2006;38:312-318.
- [3] McKee SL. An update on racing fatalities in the UK. *Equine Vet Educ* 1995;7:202-204.
- [4] Peloso JG, Mundy GD, Cohen ND. Prevalence of, and factors associated with, musculoskeletal racing injuries of Thoroughbreds. *J Am Vet Med Assoc* 1994;204:620-626.
- [5] Norrdin RW, Kawcak CE, Capwell BA, McIlwraith CW. Subchondral bone failure in an equine model of overload arthrosis. *Bone* 1998;22:133-139.
- [6] Williams RB, Harkins LS, Hammond CJ, Wood JL. Racehorse injuries, clinical problems and fatalities recorded on British racecourses from flat racing and National Hunt racing during 1996, 1997 and 1998. *Equine Vet J* 2001;33:478-486.
- [7] Johnson BJ, Stover SM, Daft BM, Kinde H, Read DH, Barr BC, Anderson M, Moore J, Woods L, Stoltz J, et al. Causes of death in racehorses over a 2 year period. *Equine Vet J* 1994;26:327-330.
- [8] McIlwraith CW, Frisbie DD, Kawcak CE, Fuller CJ, Hurtig M, Cruz A. The OARSI histopathology initiative - recommendations for histological assessments of osteoarthritis in the horse. *Osteoarthritis and cartilage / OARS, Osteoarthritis Research Society* 2010;18 Suppl 3:S93-105.
- [9] Stover SM, Murray A. The California Postmortem Program: leading the way. *Vet Clin North Am Equine Pract* 2008;24:21-36.
- [10] Parkin TD, Clegg PD, French NP, Proudman CJ, Riggs CM, Singer ER, Webbon PM, Morgan KL. Risk of fatal distal limb fractures among Thoroughbreds involved in the five types of racing in the United Kingdom. *Vet Rec* 2004;154:493-497.
- [11] Parkin TD, Clegg PD, French NP, Proudman CJ, Riggs CM, Singer ER, Webbon PM, Morgan KL. Catastrophic fracture of the lateral condyle of the third metacarpus/metatarsus in UK racehorses - fracture descriptions and pre-existing pathology. *Vet J* 2006;171:157-165.

- [12] Parkin TD, Clegg PD, French NP, Proudman CJ, Riggs CM, Singer ER, Webbon PM, Morgan KL. Analysis of horse race videos to identify intra-race risk factors for fatal distal limb fracture. *Prev Vet Med* 2006;74:44-55.
- [13] Hill AE, Stover SM, Gardner IA, Kane AJ, Whitcomb MB, Emerson AG. Risk factors for and outcomes of noncatastrophic suspensory apparatus injury in Thoroughbred racehorses. *J Am Vet Med Assoc* 2001;218:1136-1144.
- [14] Tyler TF, McHugh MP, Mirabella MR, Mullaney MJ, Nicholas SJ. Risk factors for noncontact ankle sprains in high school football players: the role of previous ankle sprains and body mass index. *Am J Sports Med* 2006;34:471-475.
- [15] Kofotolis ND, Kellis E, Vlachopoulos SP. Ankle sprain injuries and risk factors in amateur soccer players during a 2-year period. *Am J Sports Med* 2007;35:458-466.
- [16] Mohammed HO, Hill T, Lowe J. Risk factors associated with injuries in Thoroughbred horses. *Equine Vet J* 1991;23:445-448.
- [17] Cohen ND, Mundy GD, Peloso JG, Carey VJ, Amend NK. Results of physical inspection before races and race-related characteristics and their association with musculoskeletal injuries in Thoroughbreds during races. *J Am Vet Med Assoc* 1999;215:654-661.
- [18] Cohen ND, Dresser BT, Peloso JG, Mundy GD, Woods AM. Frequency of musculoskeletal injuries and risk factors associated with injuries incurred in Quarter Horses during races. *J Am Vet Med Assoc* 1999;215:662-669.
- [19] Hernandez JA, Scollay MC, Hawkins DL, Corda JA, Krueger TM. Evaluation of horseshoe characteristics and high-speed exercise history as possible risk factors for catastrophic musculoskeletal injury in thoroughbred racehorses. *Am J Vet Res* 2005;66:1314-1320.
- [20] Cohen ND, Peloso JG, Mundy GD, Fisher M, Holland RE, Little TV, Misheff MM, Watkins JP, Honnas CM, Moyer W. Racing-related factors and results of prerace physical inspection and their association with musculoskeletal injuries incurred in thoroughbreds during races. *J Am Vet Med Assoc* 1997;211:454-463.
- [21] Radtke CL, Danova NA, Scollay MC, Santschi EM, Markel MD, Da Costa Gomez T, Muir P. Macroscopic changes in the distal ends of the third metacarpal and metatarsal bones of Thoroughbred racehorses with condylar fractures. *Am J Vet Res* 2003;64:1110-1116.
- [22] Stover SM, Johnson BJ, Daft BM, Read DH, Anderson M, Barr BC, Kinde H, Moore J, Stoltz J, Ardans AA, et al. An association between complete and incomplete stress fractures of the humerus in racehorses. *Equine Vet J* 1992;24:260-263.

- [23] Eckstein F, Muller-Gerbl M, Steinlechner M, Kierse R, Putz R. Subchondral bone density in the human elbow assessed by computed tomography osteoabsorptiometry: a reflection of the loading history of the joint surfaces. *J Orthop Res* 1995;13:268-278.
- [24] Riggs CM, Whitehouse GH, Boyde A. Pathology of the distal condyles of the third metacarpal and third metatarsal bones of the horse. *Equine Vet J* 1999;31:140-148.
- [25] Nugent GE, Law AW, Wong EG, Temple MM, Bae WC, Chen AC, Kawcak CE, Sah RL. Site- and exercise-related variation in structure and function of cartilage from equine distal metacarpal condyle. *Osteoarthritis Cartilage* 2004;12:826-833.
- [26] Colahan P, Turner TA, Poulos P, Piotrowski G. Mechanical functions and sources of injury in the fetlock and carpus. Proc Annu Mtg Am Assoc Equine Practnrs 1987;689-699.
- [27] Easton KL, Kawcak CE. Evaluation of increased subchondral bone density in areas of contact in the metacarpophalangeal joint during joint loading in horses. *Am J Vet Res* 2007;68:816-821.
- [28] Brama PA, Karszenberg D, Barneveld A, van Weeren PR. Contact areas and pressure distribution on the proximal articular surface of the proximal phalanx under sagittal plane loading. *Equine Vet J* 2001;33:26-32.
- [29] Anderson TM, McIlwraith CW, Douay P. The role of conformation in musculoskeletal problems in the racing Thoroughbred. *Equine Vet J* 2004;36:571-575.
- [30] Kane AJ, Stover SM, Gardner IA, Bock KB, Case JT, Johnson BJ, Anderson ML, Barr BC, Daft BM, Kinde H, Larochelle D, Moore J, Mysore J, Stoltz J, Woods L, Read DH, Ardans AA. Hoof size, shape, and balance as possible risk factors for catastrophic musculoskeletal injury of Thoroughbred racehorses. *Am J Vet Res* 1998;59:1545-1552.
- [31] Kawcak CE, Zimmerman CA, Easton KL, McIlwraith CW, Parkin TD. Effects of third metacarpal geometry on the incidence of condylar fractures in Thoroughbred racehorses. *Am Assoc of Eq Practitioners* 2009;197.
- [32] Nunamaker DM, Butterweck DM, Provost MT. Some geometric properties of the third metacarpal bone: a comparison between the Thoroughbred and Standardbred racehorse. *J Biomech* 1989;22:129-134.
- [33] Santilli V, Frascarelli MA, Paoloni M, Frascarelli F, Camerota F, De Natale L, De Santis F. Peroneus longus muscle activation pattern during gait cycle in athletes affected by functional ankle instability: a surface electromyographic study. *Am J Sports Med* 2005;33:1183-1187.
- [34] Bennell K, Hinman R. Exercise as a treatment for osteoarthritis. *Curr Opin Rheumatol* 2005;17:634-640.

- [35] Wohl GR, Boyd SK, Judex S, Zernicke RF. Functional adaptation of bone to exercise and injury. *J Sci Med Sport* 2000;3:313-324.
- [36] Tropp H, Askling C, Gillquist J. Prevention of ankle sprains. *Am J Sports Med* 1985;13:259-262.
- [37] Verhagen E, van der Beek A, Twisk J, Bouter L, Bahr R, van Mechelen W. The effect of a proprioceptive balance board training program for the prevention of ankle sprains: a prospective controlled trial. *Am J Sports Med* 2004;32:1385-1393.
- [38] Parkin TD, Clegg PD, French NP, Proudman CJ, Riggs CM, Singer ER, Webbon PM, Morgan KL. Risk factors for fatal lateral condylar fracture of the third metacarpus/metatarsus in UK racing. *Equine Vet J* 2004;37:192-199.
- [39] Kane AJ, Stover SM, Gardner IA, Case JT, Johnson BJ, Read DH, Ardans AA. Horseshoe characteristics as possible risk factors for fatal musculoskeletal injury of Thoroughbred racehorses. *Am J Vet Res* 1996;57:1147-1152.
- [40] Kawcak CE, Bramlage LR, Embertson RM. Diagnosis and management of incomplete fracture of the distal palmar aspect of the third metacarpal bone in five horses. *J Am Vet Med Assoc* 1995;206:335-337.
- [41] McIlwraith CW. Fetlock fractures and luxations In: Nixon AJ, ed. *Equine Fracture Repair*. Philadelphia: WB Saunders Co., 1996;153-162.
- [42] Bertone AL. Distal limb: fetlock and pastern In: Hinchcliff KW, Kaneps AJ, Geor RJ, Bayly W, eds. *Equine Sports Medicine and Surgery*. China: Elsevier Ltd., 2004;289-318.
- [43] Kawcak CE, McIlwraith CW. Proximodorsal first phalanx osteochondral chip fragmentation in 336 horses. *Equine Vet J* 1994;26:392-396.
- [44] Markel MD, Martin BB, Richardson DW. Dorsal frontal fractures in the first phalanx in the horse. *Vet Surg* 1985;14:36-40.
- [45] Gillis JP, Auer JA, Holmes RE. The use of a porous bioimplant in the treatment of subchondral bone cysts in the horse. *Vet Surg* 1987;16:90.
- [46] Auer JA. Principles in fracture treatment In: Auer JA, Stick J, eds. *Equine Surgery*. 3 ed. St. Louis: Elsevier Saunders, 2006;1000-1029.
- [47] Auer JA, Schenk R. The application of tricalcium phosphate cylinders in articular and cortical defects in the horse. *Vet Surg* 1989;18:73.
- [48] Bramlage LR. Fetlock arthrodesis In: Nixon AJ, ed. *Equine Fracture Repair*. Philadelphia: W.B. Saunders Co., 1996;172-178.

- [49] Kaneps AJ, Turner TA. Diseases of the foot In: Hinchcliff KW, Kaneps AJ, Geor RJ, Bayly W, eds. *Equine Sports Medicine and Surgery*. China: Elsevier Ltd., 2004;260-288.
- [50] Frisbie DD, Al-Sobayil F, Billingham RC, Kawcak CE, McIlwraith CW. Changes in synovial fluid and serum biomarkers with exercise and early osteoarthritis in horses. *Osteoarthritis Cartilage* 2008.
- [51] Denoix JM, Audigie F. Imaging of the musculoskeletal system in horses In: Hinchcliff KW, Kaneps AJ, Geor RJ, Bayly W, eds. *Equine Sports Medicine and Surgery*. China: Elsevier Ltd., 2004;161-187.
- [52] Lloyd KC, Koblick P, Ragle C, al. E. Incomplete palmar fracture of the proximal extremity of the third metacarpal bone in horses: ten cases (1981-1986). *J Am Vet Med Assoc* 1988;192:798-803.
- [53] Tucker RL, Sande RD. Computed tomography and magnetic resonance imaging of the equine musculoskeletal conditions. *Vet Clin North Am Equine Pract* 2001;17:145-157, vii.
- [54] Muller-Gerbl M, Putz R, Kenn R. Demonstration of subchondral bone density patterns by three-dimensional CT osteoabsorptiometry as a noninvasive method for in vivo assessment of individual long-term stresses in joints. *J Bone Miner Res* 1992;7 Suppl 2:S411-418.
- [55] Les CM, Keyak JH, Stover SM, Taylor KT, Kaneps AJ. Estimation of material properties in the equine metacarpus with use of quantitative computed tomography. *J Orthop Res* 1994;12:822-833.
- [56] Gold GE, Besier TF, Draper CE, Asakawa DS, Delp SL, Beaupre GS. Weight-bearing MRI of patellofemoral joint cartilage contact area. *J Magn Reson Imaging* 2004;20:526-530.
- [57] Brechter JH, Powers CM, Terk MR, Ward SR, Lee TQ. Quantification of patellofemoral joint contact area using magnetic resonance imaging. *Magn Reson Imaging* 2003;21:955-959.
- [58] Patel VV, Hall K, Ries M, Lotz J, Ozhinsky E, Lindsey C, Lu Y, Majumdar S. A three-dimensional MRI analysis of knee kinematics. *J Orthop Res* 2004;22:283-292.
- [59] Eckstein F, Burstein D, Link TM. Quantitative MRI of cartilage and bone: degenerative changes in osteoarthritis. *NMR Biomed* 2006;19:822-854.
- [60] Eckstein F, Hudelmaier M, Wirth W, Kiefer B, Jackson R, Yu J, Eaton CB, Schneider E. Double echo steady state magnetic resonance imaging of knee articular cartilage at 3 Tesla: a pilot study for the Osteoarthritis Initiative. *Ann Rheum Dis* 2006;65:433-441.

- [61] Eckstein F, Schnier M, Haubner M, Priebsch J, Glaser C, Englmeier KH, Reiser M. Accuracy of cartilage volume and thickness measurements with magnetic resonance imaging. *Clin Orthop Relat Res* 1998;137-148.
- [62] Blemker SS, Delp SL. Three-dimensional representation of complex muscle architectures and geometries. *Ann Biomed Eng* 2005;33:661-673.
- [63] Besier TF, Gold GE, Beaupre GS, Delp SL. A modeling framework to estimate patellofemoral joint cartilage stress in vivo. *Med Sci Sports Exerc* 2005;37:1924-1930.
- [64] Shelburne KB, Torry MR, Pandy MG. Muscle, ligament, and joint-contact forces at the knee during walking. *Med Sci Sports Exerc* 2005;37:1948-1956.
- [65] Arnold AS, Salinas S, Asakawa DJ, Delp SL. Accuracy of muscle moment arms estimated from MRI-based musculoskeletal models of the lower extremity. *Comput Aided Surg* 2000;5:108-119.
- [66] Anderson DD, Goldsworthy JK, Li W, James Rudert M, Tochigi Y, Brown TD. Physical validation of a patient-specific contact finite element model of the ankle. *J Biomech* 2007;40:1662-1669.
- [67] Niebur GL, Feldstein MJ, Yuen JC, Chen TJ, Keaveny TM. High-resolution finite element models with tissue strength asymmetry accurately predict failure of trabecular bone. *J Biomech* 2000;33:1575-1583.
- [68] Keyak JH. Improved prediction of proximal femoral fracture load using nonlinear finite element models. *Med Eng Phys* 2001;23:165-173.
- [69] Crawford RP, Cann CE, Keaveny TM. Finite element models predict in vitro vertebral body compressive strength better than quantitative computed tomography. *Bone* 2003;33:744-750.
- [70] Van Rietbergen B, Muller R, Ulrich D, Ruegsegger P, Huiskes R. Tissue stresses and strain in trabeculae of a canine proximal femur can be quantified from computer reconstructions. *J Biomech* 1999;32:443-451.
- [71] Taylor D, Kuiper JH. The prediction of stress fractures using a 'stressed volume' concept. *J Orthop Res* 2001;19:919-926.
- [72] Anderson DD, Goldsworthy JK, Shivanna K, Grosland NM, Pedersen DR, Thomas TP, Tochigi Y, Marsh JL, Brown TD. Intra-articular contact stress distributions at the ankle throughout stance phase-patient-specific finite element analysis as a metric of degeneration propensity. *Biomech Model Mechanobiol* 2006;5:82-89.
- [73] Li W, Anderson DD, Goldsworthy JK, Marsh JL, Brown TD. Patient-specific finite element analysis of chronic contact stress exposure after intraarticular fracture of the tivial plafond. *J Orthop Res* 2008:1039-1045.

- [74] Jacobs CR, Eckstein F. Computer simulation of subchondral bone adaptation to mechanical loading in an incongruous joint. *Anat Rec* 1997;249:317-326.
- [75] Schileo E, Taddei F, Cristofolini L, Viceconti M. Subject-specific finite element models implementing a maximum principal strain criterion are able to estimate failure risk and fracture location on human femurs tested in vitro. *Journal of biomechanics* 2008;41:356-367.
- [76] Yosibash Z, Tal D, Trabelsi N. Predicting the yield of the proximal femur using high-order finite-element analysis with inhomogeneous orthotropic material properties. *Philos Transact A Math Phys Eng Sci* 2010;368:2707-2723.
- [77] Keyak JH, Rossi SA. Prediction of femoral fracture load using finite element models: an examination of stress- and strain-based failure theories. *J Biomech* 2000;33:209-214.
- [78] Boresi AP, Schmidt RJ. *Advanced Mechanics of Materials*. 6 ed. USA: John Wiley & Sons, 2003.
- [79] Keyak JH, Rossi SA, Jones KA, Skinner HB. Prediction of femoral fracture load using automated finite element modeling. *J Biomech* 1998;31:125-133.
- [80] Bozkus H, Karakas A, Hanci M, Uzan M, Bozdog E, Sarioglu AC. Finite element model of the Jefferson fracture: comparison with a cadaver model. *Eur Spine J* 2001;10:257-263.
- [81] Montanini R, Filardi V. In vitro biomechanical evaluation of antegrade femoral nailing at early and late postoperative stages. *Medical engineering & physics* 2010;32:889-897.
- [82] Lawrence RC, Helmick CG, Arnett FC, Deyo RA, Felson DT, Giannini EH, Heyse SP, Hirsch R, Hochberg MC, Hunder GG, Liang MH, Pillemer SR, Steen VD, Wolfe F. Estimates of the prevalence of arthritis and selected musculoskeletal disorders in the United States. *Arthritis Rheum* 1998;41:778-799.
- [83] March LM, Bachmeier CJ. Economics of osteoarthritis: a global perspective. *Baillieres Clin Rheumatol* 1997;11:817-834.
- [84] Lajeunesse D, Reboul P. Subchondral bone in osteoarthritis: a biologic link with articular cartilage leading to abnormal remodeling. *Curr Opin Rheumatol* 2003;15:628-633.
- [85] Pool RR, Meagher DM. Pathologic findings and pathogenesis of racetrack injuries. *Vet Clin North Am Equine Pract* 1990;6:1-30.
- [86] Horton WE, Jr., Bennion P, Yang L. Cellular, molecular, and matrix changes in cartilage during aging and osteoarthritis. *J Musculoskelet Neuronal Interact* 2006;6:379-381.

[87] Goldring SR, Goldring MB. Clinical aspects, pathology and pathophysiology of osteoarthritis. *J Musculoskelet Neuronal Interact* 2006;6:376-378.

CHAPTER 2  
*EX VIVO* BONE, LIGAMENT, AND TENDON STRAIN AND CONTACT PRESSURE  
IN THE EQUINE METACARPOPHALANGEAL JOINT AT WALK, TROT, AND  
GALLOP LOADS

INTRODUCTION

Injury in performance horses is of great concern to the equine practitioner. It is a major reason for the retirement and sometimes euthanasia of horses. The majority of injuries occur in the distal limb and can include both fractures and soft tissue strains and sprains. In Thoroughbred racehorses, the metacarpophalangeal joint (MCP) and the suspensory apparatus are the most commonly injured structures. At multiple racetracks in the United States, fractures of the proximal sesamoid bones and third metacarpal bone (MC III) were the most common fractures [1,2]. In the United Kingdom, lateral condylar fractures of MC III were the most common fractures [3]. These types of injuries are often catastrophic and treatment can be unrewarding. Therefore, prevention of these injuries is key.

Fatigue related damage has been shown in the MCP in the form of subchondral bone (SCB) sclerosis, cartilage erosion, and wear lines [4-6]. Many factors may play a role in these degenerative and maladaptive processes including the biomechanical environment in and surrounding the joint. This environment is influenced by many

factors including cartilage, ligament, and tendon shape and stiffness, and bone geometry and material properties. Understanding this environment is important since even slight alterations due to subclinical to mild injuries can increase the risk of musculoskeletal injury [7].

Various studies have evaluated ligament and tendon strain [8-11], bone strain [12-15], and joint surface pressure distribution [16,17] in the MCP and surrounding structures. Strains in both the bones and soft tissue structures increased with increasing load [12]. Contact pressure as well as the area in contact between the articulating surfaces was also found to increase with increasing load [16-18]. However, all of these studies only looked at a few components at a time as opposed to determining all of these parameters within a single limb. Because of variations in loading schemes between different studies, it is difficult to determine how all of the data from the literature fits together.

Understanding the biomechanical forces to which the joint and its supporting structures are subjected is important in being able to elucidate possible mechanisms of injury. The objective of this study was to provide a comprehensive dataset of ligament and tendon strain, bone strain, and pressure distribution in the MCP and its supporting structures. In addition, the data from this study will be used for the validation of a finite element (FE) model of the MCP that can be used to determine parameters such as stress within the joint which cannot be experimentally measured. It was hypothesized that the strains as well as the contact pressure would increase with increasing load. Because all of the current methods available to measure contact pressure require the disruption of the joint capsule, the ligament and tendon strain was measured both before and after

arthrotomy. This was done in order to determine the effect of arthrotomy on ligament and tendon strain. It was hypothesized that this disruption to the integrity of the capsule would significantly affect the strains seen in the ligaments and tendons surrounding the MCP. Furthermore, the specific change (increase, decrease, or no change in strain) would depend on the individual ligament and its location relative to the center of the joint.

## MATERIALS AND METHODS

Eight forelimbs from eight different horses were used in this study. The horses were selected from those presented to the necropsy service at the Colorado State University Veterinary Medical Center as well as from other research projects not associated with the current study.

The forelimbs were removed within 2 – 36 hours of euthanasia. The humerus was cut transversely distal to the deltoid tuberosity and the forelimbs were stored at -20°C until testing. Prior to testing, the limbs were thawed at room temperature for 48 hours. The hoof and humerus were potted in customized molds using DynaCast (Kindt-Collins Co., Cleveland, OH). The MCP was skinned and hydration was maintained by spraying the limb with 0.9% saline every 15 minutes.

### *General loading protocol*

The humerus was placed in a specially designed jig that mounts to the actuator of a materials testing system (MTS, model 809, MTS Systems Corporation, Eden Prairie,

MN) and the hoof was placed in a specially designed jig that mounts to the load cell platen of the MTS. A 45 kN capacity load cell (model MC5.4641, Advanced Mechanical Technology, Inc., Watertown, MA) with 6 degrees of freedom was used.

Loading was based on MCP angle as measured between the dorsal aspect of MC III and the proximal phalanx: 144° (walk), 128° (trot), and 120° (gallop) [19]. The displacements required to achieve the given MCP angle were determined by measuring the MCP angle with a goniometer while loading the limb. After preconditioning the limb for 20 cycles from unloaded to maximum displacement at 1 Hz, the limb was loaded on the MTS at a rate of 85 mm/s under displacement control to the given displacements. The limb was held at the given displacement for 5 seconds, returned to zero displacement, and held for 5 seconds. Five cycles of data were collected at 100 Hz for each displacement before moving on to the next displacement. The order in which the displacements were done was randomized.

#### *Ligament and tendon strain*

Differential variable reluctance transformers with 3 mm (M-DVRT-3, MicroStrain, Inc., Williston, VT) and 6 mm (M-DVRT-6, MicroStrain, Inc., Williston, VT) gauge lengths were placed in the ligaments and tendons listed in Table 2.1. The initial length ( $L_0$ ) of the transducers was measured with digital calipers before testing. Ligament and tendon strain ( $\epsilon$ ) was calculated by dividing the change in length ( $\Delta L$ ) by the initial length:  $\epsilon = \Delta L/L_0$ . Because only 6 DVRTs were available, the above loading procedure was repeated 3 times in order to collect data from all 16 ligament/tendon locations.

**Table 2.1:** Ligaments and tendons where DVRTs were placed to measure ligament/tendon strain.

<b>Ligaments and Tendons</b>		
SDFT: proximal to MCP joint	SL: main branch	Medial oblique sesamoidean
SDFT: distal medial branch	SL: medial branch	Lateral oblique sesamoidean
SDFT: distal lateral branch	SL: lateral branch	Medial annular
DDFT: proximal to MCP joint	SL: medial extensor branch	Lateral annular
Straight sesamoidean	SL: lateral extensor branch	Medial collateral
		Lateral collateral

SDFT: superficial digital flexor tendon; DDFT: deep digital flexor tendon; SL: suspensory ligament.

*Summary of data collection*

Two joint conditions were investigated for each limb: intact and disrupted joint. In the intact condition, differential variable reluctance transformers (DVRTs) were placed in 16 ligaments and tendons surrounding the MCP. After testing the limbs in the intact condition using the above protocol, the lateral and common digital extensors were transected and the long fibers of the medial and lateral collateral ligaments were longitudinally incised and elevated off of the bone. The joint capsule was opened on the dorsal aspect taking care not to disrupt the collateral ligaments. This joint disruption was done in order to allow for the placement of rosette strain gauges on MC III and the proximal phalanx and the insertion of a pressure mapping sensor in the joint. The loading procedure described above was then repeated for the disrupted joint condition.

### *Bone strain*

Bone strain was recorded from a total of six locations. Rectangular stacked rosette strain gauges (C2A-06-062WW-350, Vishay Micro-Measurements, Raleigh, NC) were placed on the dorsomedial and dorsolateral aspects of MC III (dm\_mc3, dl\_mc3) and the proximal phalanx (dm\_p1, dl\_p1) just proximal and distal respectively to the articular surface. One was also placed on the medial and lateral aspects of MC III (med\_mc3, lat\_mc3) under the incised and elevated collateral ligaments (Figure 2.1). The collateral ligaments were incised longitudinally and elevated off of the bone for the attachment of the strain gauges as opposed to completely transecting them in order to minimize the disruption to the joint and its supporting structures.

The principal bone strains ( $\epsilon_p$  and  $\epsilon_q$ ) were calculated using the following equation:

$$\epsilon_{p,q} = \frac{\epsilon_1 + \epsilon_3}{2} \pm \frac{1}{\sqrt{2}} \sqrt{(\epsilon_1 - \epsilon_2)^2 + (\epsilon_2 - \epsilon_3)^2}$$

where  $\epsilon_1$ ,  $\epsilon_2$ , and  $\epsilon_3$  are the strains sensed by each of the 3 individual strain gauges on the rosette [20].

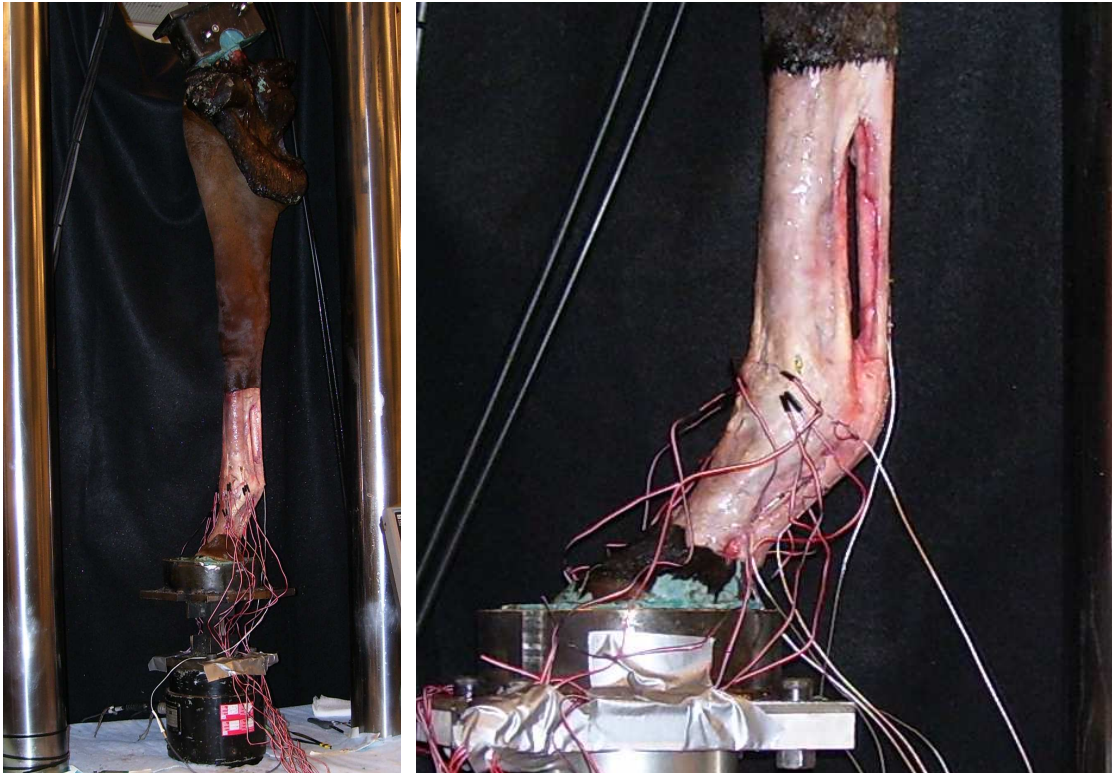


**Figure 2.1:** Photographs of the limb on the materials testing system with strain gages and DVRTs attached.

### *Contact pressure*

A pressure mapping sensor (model 6900-10K, Tekscan, Boston, MA) was placed between MC III and the proximal phalanx as well as between MC III and the proximal sesamoid bones. The sensor was equilibrated and calibrated on an MTS machine. For equilibration, the sensor was placed between two flat loading platens. The loading platens had a piece of stiff foam on the surface to simulate the articular cartilage. Two point calibration was performed with the sensor placed between a cylinder and a conforming block (again with foam) in order to simulate the curvature of the condyles.

The sensor had 4 sensing areas. Two were placed on the medial and lateral condyles with one edge at the most dorsal aspect of the articular surface of MC III and

the rest of the sensor continuing in the palmar direction in order to determine the contact pressure between MC III and the proximal phalanx. The other two were placed on the medial and lateral condyles with one edge at the level of the transverse ridge and the rest of the sensor continuing in the palmar direction in order to determine contact pressure between MC III and the proximal sesamoid bones.

While there are inherent errors associated with any type of pressure measurement system and inaccuracies due to the required disruption of the joint integrity to insert the device, there is at present no satisfactory *in vivo* method of directly measuring pressure distribution within a joint. The use of a pressure measurement system represents one of the methods currently used to estimate these parameters [21].

#### *Data collection and analysis*

Force ( $F_x$ ,  $F_y$ ,  $F_z$ ), limb displacement, DVRT displacement, and bone strain data were collected at 100 Hz using a custom written program designed in LabView (National Instruments, Austin, TX). Data was filtered using a low pass second order Butterworth filter with a 5 Hz cutoff [22]. The means for the 5 second holds for each of the 5 cycles for each displacement were calculated.

Analysis of the mean strain for each ligament and tendon as well as the force data was done using an ANOVA with joint condition (intact, disrupted) and displacement (walk, trot, gallop) as fixed factors and horse and horse by condition as random factors. The interaction between condition and displacement was included in the model if it was found to be significant. Positive strain indicates that the ligament or tendon is being stretched.  $F_x$  is the force in the dorsopalmar direction with positive being towards the

dorsal aspect.  $F_y$  is the force in the mediolateral direction with positive being towards the medial aspect. The sign was reversed for left forelimbs in order to conform to this coordinate system.  $F_z$  is force in the proximodistal direction with negative indicating compression of the limb (Figure 2).

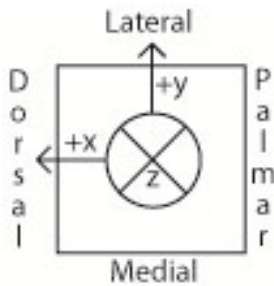


**Figure 2.2:** Diagram of coordinate system for force data.

An ANOVA was also used to compare the effect of side (medial or lateral) for the annular, collateral, extensor branches of the suspensory, oblique sesamoidean, and suspensory ligaments, and distal superficial digital flexor tendon (SDFT) within a joint condition. For the latter two structures, axial was also included. In this analysis, strain was the outcome parameter, displacement and side were included as fixed factors, and horse and horse by displacement were included as random factors. The interaction between displacement and side was included in the model if it was found to be significant.

Principal bone strain and direction were analyzed similarly except the joint condition factor was omitted. Horse by displacement was included as a random factor initially, but was found not to be significant and was therefore excluded in the final analysis. Horse was the only random factor included. Significance was set at  $p < 0.05$ . Data is reported as means  $\pm$  standard error (s.e.).

Contact pressure data from the Tekscan sensor was collected at 60 Hz using I-Scan (version 5.90, Tekscan Inc., Boston, MA). The average and peak pressure for the 5 second holds for each of the 5 cycles for each displacement were calculated for each of the 4 sensing areas. Average and peak pressure were analyzed similarly to bone strain with displacement as a fixed factor and horse as a random factor.

## RESULTS

Eight forelimbs, 4 right and 4 left, from 8 different horses were used in this study (Table 2.2). Mean age and weight with standard deviation were  $5.1 \pm 1.6$  years (range 2.5 – 7) and  $421 \pm 63$  kg (range 340 – 499) respectively.

**Table 2.2:** Demographic data for horses used in the *ex vivo* mechanical testing.

Horse	Age	Sex	Weight (kg)	Limb
1	7 years	Male	386 <sup>a</sup>	Left
2	7 years	Gelding	Unknown	Left
3	5 years	Unknown	340 <sup>a</sup>	Left
4	6 years	Gelding	408 <sup>a</sup>	Right
5	2.5 years	Female	363	Left
6	5 years	Gelding	499	Right
7	4.5 years	Female	476	Right
8	3.5 years	Female	476	Right

a: weights approximated

There was a significant displacement effect for Fx, Fy, and Fz ( $p < 0.0001$ ). Force increased with increasing displacement. Means pooled over condition and standard deviations are reported in Table 2.3.

**Table 2.3:** Means and standard errors for the force data at the different displacements.

	Walk	Trot	Gallop
Fx	-154.86 ± 24.47 <sup>a</sup>	-311.67 ± 30.42 <sup>b</sup>	-385.66 ± 33.41 <sup>c</sup>
Fy	18.13 ± 8.58 <sup>a</sup>	75.93 ± 15.49 <sup>b</sup>	120.56 ± 20.63 <sup>c</sup>
Fz	-1785.84 ± 159.94 <sup>a</sup>	-3410.86 ± 152.14 <sup>b</sup>	-4568.64 ± 139.75 <sup>c</sup>

Different superscripts indicate significant differences ( $p < 0.0001$ ) between the displacements within the force measurement.

### *Ligament and tendon strain*

All of the ligaments and tendons had positive strain values except the medial and lateral collateral ligaments. There was a significant displacement effect for all of the ligaments and tendons. There was a trend for a displacement by condition effect for the lateral oblique ligament ( $p = 0.0576$ ). However, displacement by condition and condition were not significant at  $p < 0.05$  for any of the ligaments or tendons. Therefore, the means for the two conditions were pooled (Figure 2.3).

For the intact and disrupted joint conditions, the displacement by side interaction was significant for the SDFT ( $p = 0.0003$ ,  $p = 0.002$  respectively). Strain was greater on the medial side compared to the lateral side except for at the walk load in the disrupted joint condition. The effect of side was not significant for any of the other soft tissue structures in the intact joint condition. For the disrupted joint condition, there was also a significant side effect for the annular ligaments ( $p < 0.0001$ ) and the extensor branches of the suspensory ligament ( $p = 0.004$ ). Strain was again greater on the medial side compared to the lateral side for all loads.

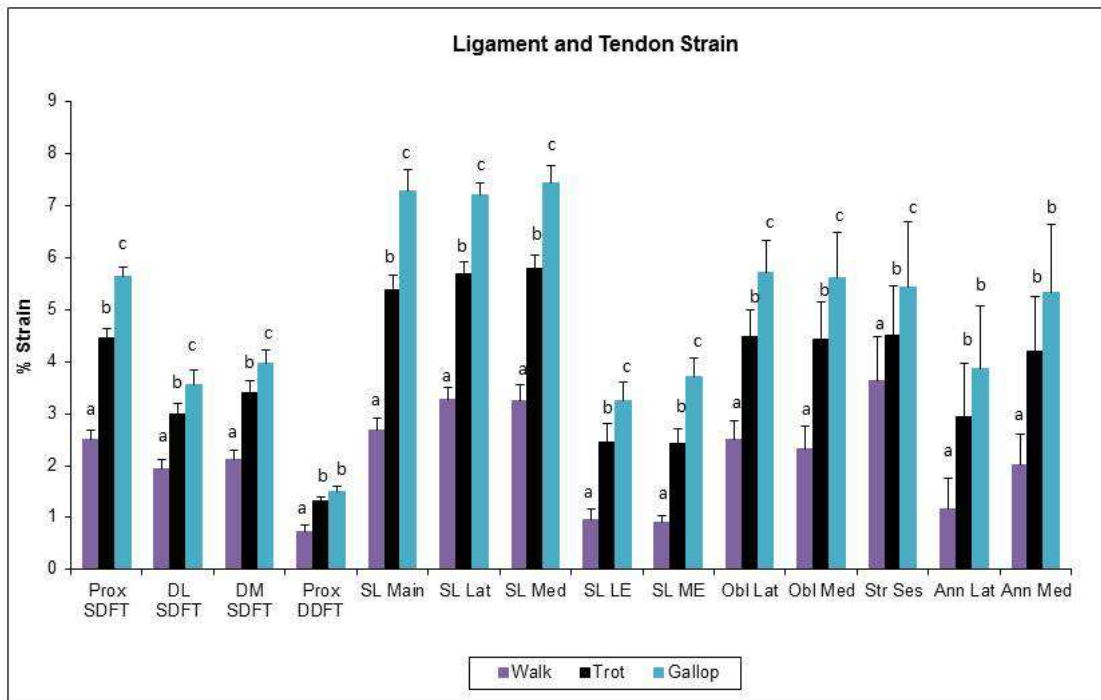


**Figure 2.3:** Graph of mean ligament and tendon strains  $\pm$  s.e. Prox: proximal; DL: distal lateral; DM: dorsal medial; Lat: lateral; Med: medial; LE: lateral extensor; ME: medial extensor; OBL: oblique sesamoidean; Str Ses: straight sesamoidean; Ann: annular; Different letters indicate significant differences ( $p < 0.05$ ) between the displacements within a given ligament or tendon.

### *Bone strain*

The largest principal bone strain was compressive for all locations except the dorsolateral MC III at the walk displacement (Figure 2.4). There was a significant displacement effect for all bone locations. In addition, there was a significant displacement by side interaction for the proximal phalanx and the maximum principal strain on the dorsal aspect of MC III. For the dorsal and abaxial aspects of MC III, the maximum and minimum principal strains were higher on the medial side in comparison to the lateral side. For the dorsal proximal phalanx, the strains were higher on the lateral side.

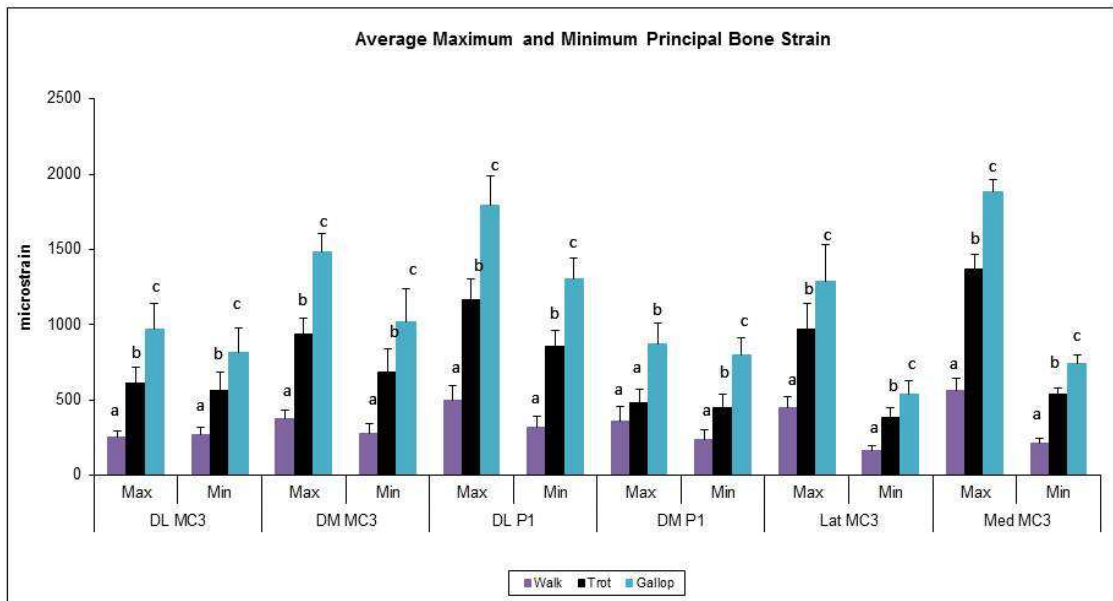


**Figure 2.4:** Graph of the mean principal bone strain  $\pm$  s.e. Max is the compressive bone strain; Min is the tensile bone strain. DL: dorsal lateral; DM: dorsal medial; Lat: lateral; Med: medial; P1: proximal phalanx. Different letters indicate significant differences ( $p < 0.05$ ) between the displacements within a given bone location and principal strain.

### Contact pressure

The recordings for the two sensing areas placed on the palmar aspect of MC III cut out in 4 limbs (horses 2, 4, 7, and 8) due to pinching of the sensor where it exited the dorsal aspect of the joint. Even with repositioning and replacement of the sensor, recordings could not be obtained in these limbs. Therefore, statistics for the palmar aspect indicated as LPSB and MPSB were performed excluding these limbs.

Average (Figure 2.5) and peak (Figure 2.6) pressures increased with increasing load. The displacement effect was significant for the dorsomedial and dorsolateral aspect of MC III (MP1 and LP1) as well as the palmar medial aspect of MC III (MPSB). For the palmar lateral aspect, displacement was only significant for peak pressure (LPSB). Figure 2.7 shows the pressure distribution pattern between MC III and the proximal

sesamoid bones at the gallop load. The abaxial, axial, and palmar regions had the highest pressures while the central and transverse regions had the lowest pressures.

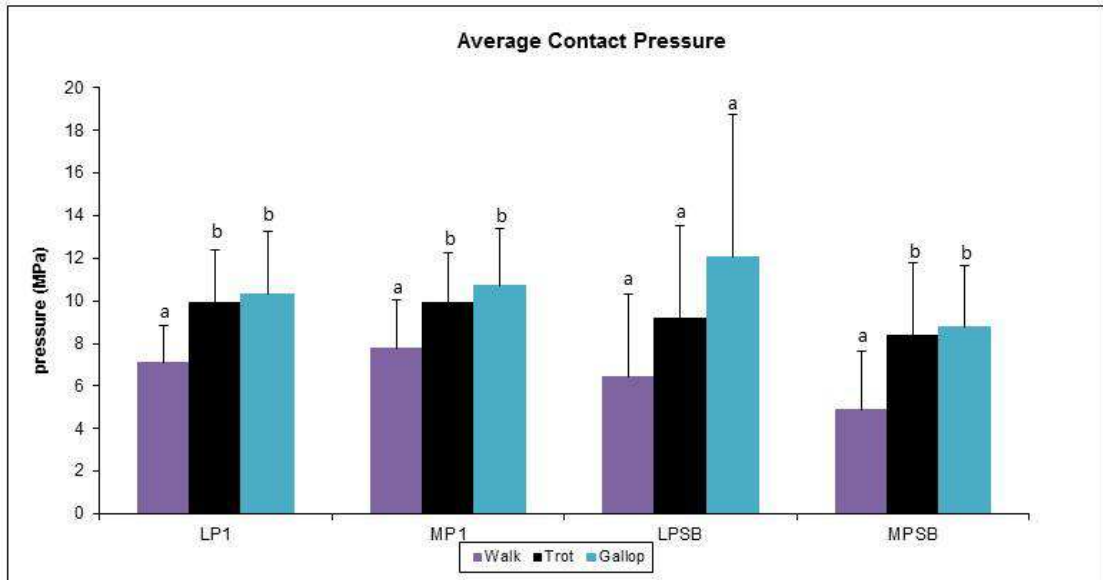


**Figure 2.5:** Graph of average contact pressure + s.e. on the distal condyles of MC III for four areas: dorsolateral (LP1), dorsomedial (MP1), palmar lateral (LPSB), and palmar medial (MPSB) at walk, trot, and gallop loads. Different letters indicate significant differences ( $p < 0.05$ ) between the displacements within a given location.

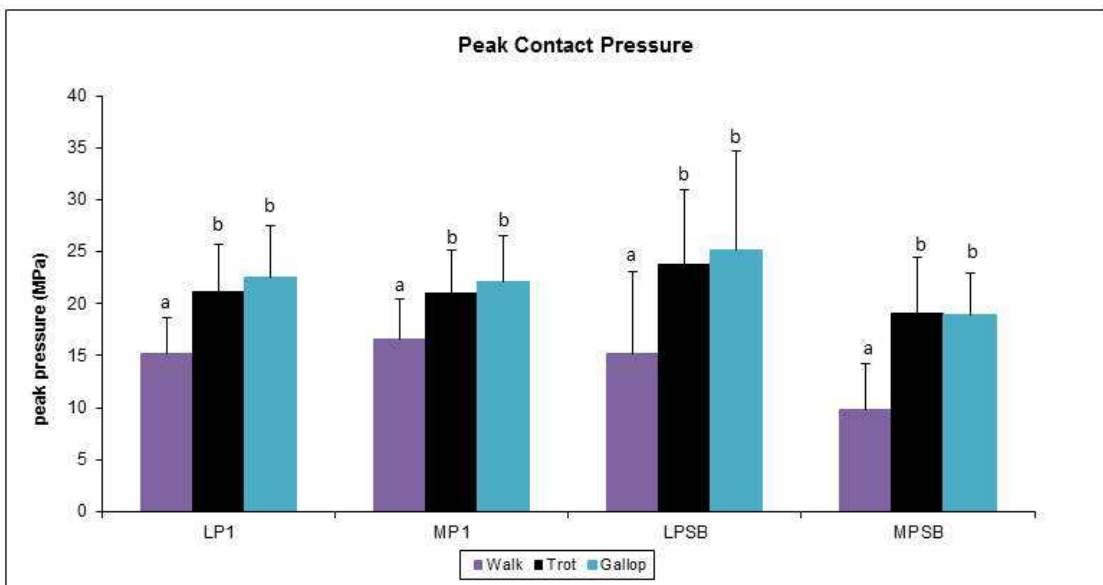


**Figure 2.6:** Graph of peak contact pressure + s.e. on the distal condyles of MC III for four areas: dorsolateral (LP1), dorsomedial (MP1), palmar lateral (LPSB), and palmar medial (MPSB) at walk, trot, and gallop loads. Different letters indicate significant differences ( $p < 0.05$ ) between the displacements within a given location.

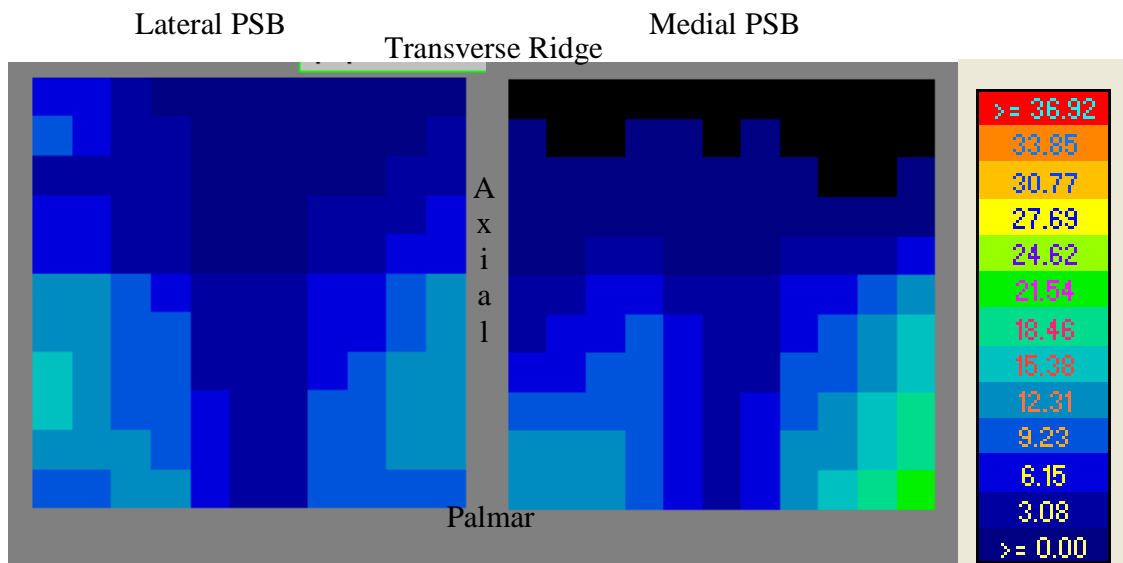


**Figure 2.7:** Representative image of the pressure distribution on MC III due to contact with the proximal sesamoid bones at the gallop load. Scale is in MPa.

## DISCUSSION

Significant differences were found in ligament and tendon strain as the limbs were loaded at walk, trot, and gallop displacements. Crevier-Denoix et al. [23] found that the strain at failure for the SDFT was 12.3% and 9.9% for normal and diseased tendons respectively. The value of 5.6% strain found in this study for the SDFT at the gallop displacement is well within the viscoelastic range of the normal tendon. However, there is a much smaller safety factor if the tendon is diseased. During a race, especially at the end when fatigue is the greatest and larger magnitude strains can be expected, the strains could easily fall within the plastic range particularly in those horses that are already suffering from mild or even subclinical injuries.

The strains for the SDFT, deep digital flexor tendon (DDFT), suspensory ligament (SL) and straight sesamoidean ligament in the current study compared well to that previously published. The current study found strains ranging from 2.5% to 5.6% in the SDFT under loads ranging from 1785 – 4568 N. Riemersma [24] recorded strains of approximately 4% at 2700 N to 6% at 5400 N in the hindlimb SDFT. Strain in the SDFT in the forelimb was 2.19% at the walk and 4.15% at the trot in ponies [10]. Shoemaker et al. [25] found a 3.5% increase when the limb was loaded from 890 N to 3115 N.

In the SL, strains up to 10% have been recorded with loads as great as 2.5 kN in the main branch [26]. Under loads similar to the gallop load in this study, Swanstrom et al. [26] found strains to be approximately 5-6%. These values are a little lower than that found in this study (7.3%). However, there were some differences in testing protocol. In Swanstrom's study, the SL was isolated and tested in a bone – ligament – cryoclamp setup under a strain rate of 2 Hz. In the current study, the strain in the SL was recorded with the limb intact from hoof to humerus. Because of the size of the limb, there were limitations in the loading rate that the MTS could achieve. The loading rate was therefore closer to 1.2 Hz. The slower loading rate could account for the higher strain values.

For the medial and lateral branches of the SL, Le Jeune et al. [12] found strains ranging from 2-6% and 4-8% respectively under loads from 3000-5600 N. In comparison, strains ranging from 3-7% were found for both the medial and lateral SL in the current study.

Swanstrom et al. [26] recorded approximately 4% strain at 4500 N and up to 10% at 8000 N in the straight sesamoidean ligament. The current study at the gallop load, which is similar to the 4500 N load of Swanstrom's study, found the strain to be 5.4%.

Strain values for the DDFT, which ranged from 0.73% to 1.48%, were lower than that of the SDFT. Studies vary in the values that have been recorded for the DDFT. Riemersma [10] found strain values of 1.15% and 1.7% for the walk and trot respectively in ponies. Shoemaker et al. [25] found an increase in strain of 1.4% when the load was increased from 890 N to 3115 N. The values are relatively similar despite differences in testing parameters.

Similar to the study by Le Jeune et al. [12], the maximum principal strain was compressive for the dorsal aspect of MC III (except dorsolateral MC III at the walk in the current study). The strains for the abaxial aspect of MC III were also compressive. However in Le Jeune's study only a uniaxial strain gauge was used so principal strains were not calculated. The values are similar, though tend to be higher, in general for the walk and trot loads and lower for the gallop load in the current study compared to Le Jeune's study. In comparing loading protocols, this difference is not surprising. The loads in the current study were 1785 N, 3410 N, and 4568 N compared to 1400 N, 3000 N, and 5600 N in Le Jeune's study. In addition, the investigators in the prior study completely transected the long fibers of the collateral ligaments and reported values as a change from the standing load defined as 890 N so differences are expected.

The side (medial vs. lateral) differences appear to vary based on if the structure is proximal or distal to the joint. The strain tended to be greater on the medial side proximal to the joint space and greater on the lateral side distal to the joint space for the

bone strain. For the soft tissue structures, the strain was greater on the medial side for all of the ligaments and tendons except for the extensor branches of the suspensory ligament and the annular ligaments in the intact joint condition. In the disrupted joint condition, the soft tissue strain was greater on the medial side for all of the structures.

Similar to the studies by Brahma et al. [16] and Colahan et al. [17], the surface contact pressure was found to increase with increasing load. Brahma et al. reported mean pressures ranging from 5 – 35 MPa and peak pressures as high as 45 MPa for the proximal phalanx. In the current study, values were much lower, 7-10 MPa and 22 MPa for mean and peak pressures respectively. However, there were a number of differences between the two studies. In the current study, a dynamic sensor was placed on two discrete areas on the dorsal aspect of the medial and lateral condyles of MC III whereas in the study by Brahma et al., pressure film was placed on the entire articulating surface of the proximal phalanx. In addition, the loads in the latter study were much higher ranging from 1800 to 12,000 N.

Studies investigating the effect of cyclic loading on cartilage have shown that chondrocyte apoptosis can occur with cyclic loading as low as 5-6 MPa [27,28]. D’Lima et al. [29] showed that an impact load of 14 MPa resulted in a significant increase in both glycosaminoglycan release and chondrocyte apoptosis compared to non-loaded control cartilage explants. In addition, failure of the superficial cartilage layer has been shown to occur at 14-59 MPa in bovine tissue samples [30]. The peak pressure of 22 MPa found in this study could result in the initiation of cartilage damage and degradation. Repetition of these loads on already damaged tissue could progress to severe damage and lead to osteoarthritis in a relatively young racehorse.

To the author's knowledge, this is the first study to measure surface contact pressure between the distal condyles of MC III and the proximal sesamoid bones. Similar to the proximal phalanx, pressure increased with increasing load. However, the relative increase in mean and peak pressure was much greater for the proximal sesamoid bones. There was a 70% (mean) and 95% (peak) and a 42% (mean) and 56% (peak) increase in pressure for the medial and lateral proximal sesamoid bones respectively as the load increased from walk to gallop. In comparison, the percent increase in the mean and peak pressures for the medial (28% and 26%) and lateral (39% and 40%) aspect of the articulating surface of the proximal phalanx was much lower. The relatively greater increase in pressure over a smaller area may help to explain the higher incidence of fracture in the proximal sesamoid bones in comparison to the proximal phalanx.

In evaluating the pressure distribution pattern between MC III and the proximal sesamoid bones, the highest pressures were found axially and abaxially especially towards the palmar aspect leaving a relatively low pressure area in the center (Figure 2.7). This pressure distribution pattern may lead to an area of high tension in the parasagittal groove region where many condylar fractures are thought to initiate.

Confounding the data is the fact that collecting data for the open joint capsule always occurred after the intact joint condition by the nature of the problem. Although the limb was preconditioned, strains could have been varied simply due to the ligaments being more warmed up after having gone through the intact testing. However when comparing the intact to the disrupted joint condition, there were some soft tissue structures that showed an increase in strain while others showed a decrease in strain when the joint was opened. This suggests that the limbs were sufficiently preconditioned. In

future studies however, it would be ideal to test both forelimbs from a given horse and randomly assign one to the intact condition and the other to the disrupted joint condition group. As is the case with the majority of cadaver studies, the variation between specimens is generally great leading to large standard deviations. Although the condition effect was not significant, there were consistent changes suggesting that opening the joint capsule may indeed have an effect on the mechanics of the joint. This may have implications for arthrotomies. Even though the joint capsule is sutured, the mechanics of the joint may be affected while the capsule is healing. By testing both limbs from a given horse, and increasing the sample size, the variability may be reduced allowing for a greater sensitivity in determining the effect of opening the joint capsule. In any case, further studies are warranted. To further investigate the sequential effect of testing, after testing the limbs in the intact group, the joint capsule could be opened in these limbs and the testing repeated. This data could then be compared to the data from the limbs in the disrupted joint group. In future studies, it would also be interesting to investigate the effect of opening the joint capsule on not only soft tissue strain, but on bone strain as well.

Many simplifying assumptions are made in the development of FE models. For example, most models do not include the joint capsule. However, opening the joint capsule may change the joint dynamics. While these simplifying assumptions are generally necessary due to computational limitations, it is important to realize the limitations of the model and how these assumptions can affect the predictions obtained from such models.

In conclusion, the results from this study support the hypotheses that strain and contact pressure increases with increasing load and that further investigation of the effect of disruption of the joint capsule is warranted. In addition, the loading distribution pattern on the proximal sesamoid bones provides insight into the high incidence of injury in these bones. The peak pressures seen especially at the higher loads may also help to explain the damage that can be seen within the joint in relatively young horses.

## REFERENCES

- [1] Estberg L, Stover SM, Gardner IA, Johnson BJ, Case JT, Ardans A, Read DH, Anderson ML, Barr BC, Daft BM, Kinde H, Moore J, Stoltz J, Woods LW. Fatal musculoskeletal injuries incurred during racing and training in Thoroughbreds. *J Am Vet Med Assoc* 1996;208:92-96.
- [2] Johnson BJ, Stover SM, Daft BM, Kinde H, Read DH, Barr BC, Anderson M, Moore J, Woods L, Stoltz J, et al. Causes of death in racehorses over a 2 year period. *Equine Vet J* 1994;26:327-330.
- [3] Parkin TD, Clegg PD, French NP, Proudman CJ, Riggs CM, Singer ER, Webbon PM, Morgan KL. Risk of fatal distal limb fractures among Thoroughbreds involved in the five types of racing in the United Kingdom. *Vet Rec* 2004;154:493-497.
- [4] Radtke CL, Danova NA, Scollay MC, Santschi EM, Markel MD, Da Costa Gomez T, Muir P. Macroscopic changes in the distal ends of the third metacarpal and metatarsal bones of Thoroughbred racehorses with condylar fractures. *Am J Vet Res* 2003;64:1110-1116.
- [5] Parkin TD, Clegg PD, French NP, Proudman CJ, Riggs CM, Singer ER, Webbon PM, Morgan KL. Catastrophic fracture of the lateral condyle of the third metacarpus/metatarsus in UK racehorses - fracture descriptions and pre-existing pathology. *Vet J* 2006;171:157-165.
- [6] Riggs CM, Whitehouse GH, Boyde A. Pathology of the distal condyles of the third metacarpal and third metatarsal bones of the horse. *Equine Vet J* 1999;31:140-148.
- [7] Hill AE, Stover SM, Gardner IA, Kane AJ, Whitcomb MB, Emerson AG. Risk factors for and outcomes of noncatastrophic suspensory apparatus injury in Thoroughbred racehorses. *J Am Vet Med Assoc* 2001;218:1136-1144.
- [8] Crevier N, Pourcelot P, Denoix JM, Geiger D, Bortolussi C, Ribot X, Sanaa M. Segmental variations of in vitro mechanical properties in equine superficial digital flexor tendons. *Am J Vet Res* 1996;57:1111-1117.
- [9] Lochner FK, Milne DW, Mills EJ, Groom JJ. In vivo and in vitro measurement of tendon strain in the horse. *Am J Vet Res* 1980;41:1929-1937.
- [10] Riemersma DJ, van den Bogert AJ, Jansen MO, Schamhardt HC. Tendon strain in the forelimbs as a function of gait and ground characteristics and in vitro limb loading in ponies. *Equine Vet J* 1996;28:133-138.
- [11] Jansen MO, Schamhardt HC, van den Bogert AJ, Hartman W. Mechanical properties of the tendinous equine interosseus muscle are affected by in vivo transducer implantation. *J Biomech* 1998;31:485-490.

- [12] Le Jeune SS, Macdonald MH, Stover SM, Taylor KT, Gerdes M. Biomechanical investigation of the association between suspensory ligament injury and lateral condylar fracture in thoroughbred racehorses. *Vet Surg* 2003;32:585-597.
- [13] Les CM, Stover SM, Taylor KT, Keyak JH, Willits NH. Ex vivo simulation of in vivo strain distributions in the equine metacarpus. *Equine Vet J* 1998;30:260-266.
- [14] Davies HM, McCarthy RN, Jeffcott LB. Surface strain on the dorsal metacarpus of Thoroughbreds at different speeds and gaits. *Acta Anat* 1993;146:148-153.
- [15] Gross TS, McLeod KJ, Rubin CT. Characterizing bone strain distributions in vivo using three triple rosette strain gages. *J Biomech* 1992;25:1081-1087.
- [16] Brama PA, Karszenberg D, Barneveld A, van Weeren PR. Contact areas and pressure distribution on the proximal articular surface of the proximal phalanx under sagittal plane loading. *Equine Vet J* 2001;33:26-32.
- [17] Colahan P, Turner TA, Poulos P, Piotrowski G. Mechanical functions and sources of injury in the fetlock and carpus. Proc Annu Mtg Am Assoc Equine Practnrs 1987;689-699.
- [18] Easton KL, Kawcak CE. Evaluation of increased subchondral bone density in areas of contact in the metacarpophalangeal joint during joint loading in horses. *Am J Vet Res* 2007;68:816-821.
- [19] McGuigan MP, Wilson AM. The effect of gait and digital flexor muscle activation on limb compliance in the forelimb of the horse *Equus caballus*. *J Exp Biol* 2003;206:1325-1336.
- [20] Murray WM, Miller WR. *The Bonded Electrical Resistance Strain Gage*. New York: Oxford University Press, Inc., 1992.
- [21] Wu JZ, Herzog W, Epstein M. Effects of inserting a pressensor film into articular joints on the actual contact mechanics. *J Biomech Eng* 1998;120:655-659.
- [22] Winter DA. *Biomechanics and Motor Control of Human Movement*. 3rd ed. New Jersey: John Wiley & Sons, Inc., 2005.
- [23] Crevier-Denoix N, Ruel Y, Dardillat C, Jerbi H, Sanaa M, Collobert-Laugier C, Ribot X, Denoix JM, Pourcelot P. Correlations between mean echogenicity and material properties of normal and diseased equine superficial digital flexor tendons: an in vitro segmental approach. *J Biomech* 2005;38:2212-2220.
- [24] Riemersma DJ, Schamhardt HC. In vitro mechanical properties of equine tendons in relation to cross-sectional area and collagen content. *Res Vet Sci* 1985;39:263-270.

- [25] Shoemaker RS, Bertone AL, Mohammad LN, Arms SW. Desmotomy of the accessory ligament of the superficial digital flexor muscle in equine cadaver limbs. *Vet Surg* 1991;20:245-252.
- [26] Swanstrom MD, Zarucco L, Hubbard M, Stover SM, Hawkins DA. Musculoskeletal modeling and dynamic simulation of the thoroughbred equine forelimb during stance phase of the gallop. *J Biomech Eng* 2005;127:318-328.
- [27] Islam N, Haqqi TM, Jepsen KJ, Kraay M, Welter JF, Goldberg VM, Malesud CJ. Hydrostatic pressure induces apoptosis in human chondrocytes from osteoarthritic cartilage through up-regulation of tumor necrosis factor-alpha, inducible nitric oxide synthase, p53, c-myc, and bax-alpha, and suppression of bcl-2. *J Cell Biochem* 2002;87:266-278.
- [28] Clements KM, Bee ZC, Crossingham GV, Adams MA, Sharif M. How severe must repetitive loading be to kill chondrocytes in articular cartilage? *Osteoarthritis and cartilage / OARS, Osteoarthritis Research Society* 2001;9:499-507.
- [29] D'Lima DD, Hashimoto S, Chen PC, Colwell CW, Jr., Lotz MK. Human chondrocyte apoptosis in response to mechanical injury. *Osteoarthritis and cartilage / OARS, Osteoarthritis Research Society* 2001;9:712-719.
- [30] Kerin AJ, Wisnom MR, Adams MA. The compressive strength of articular cartilage. *Proceedings of the Institution of Mechanical Engineers Part H, Journal of engineering in medicine* 1998;212:273-280.

CHAPTER 3  
DEVELOPMENT AND VALIDATION OF A THREE DIMENSIONAL FINITE  
ELEMENT MODEL OF THE EQUINE METACARPOPHALANGEAL JOINT

INTRODUCTION

Catastrophic injury of the equine metacarpophalangeal joint (MCP) is a major concern to the equine practitioner working with racehorses. Musculoskeletal injuries of the MCP in general are a major reason for retirement and euthanasia in racehorses. Lateral condylar fractures of the third metacarpal bone (MC III) [2,3] and fractures of the proximal sesamoid bones [4,5] are the most common types of fractures. Many times these fractures are not able to be fixed and the most humane decision is euthanasia on the racetrack.

With all of the possible variations in loading parameters such as magnitude, rate, and repetitiveness, combined with patient conformation, gait patterns, loading history, and neuromuscular variations, the study of causative factors of fracture and injury is difficult at best. The use of computer models provides a method of investigating individual variables separately and in conjunction by allowing the user to change parameters such as bone geometry, joint laxity, and material properties. In this way, parameters that show promise of having major effects on prevention or predisposition to

injury and disease can be determined thus narrowing the possibilities without having to sacrifice large numbers of animals for controlled experimental studies. In addition, it can assist in determining what information is important to record in prospective studies.

Finite element (FE) modeling has been used to study a multitude of problems. They can assist in predicting bone strength and fracture risk [6-8]. When based on computed tomography (CT) and/or magnetic resonance imaging (MRI) data, FE models can provide a non-invasive *in vivo* method of determining contact and pressure distribution patterns within a joint [9]. While FE models of other equine structures such as the MC III [10], the radius [11], and the hoof [12-14] have been developed, to the author's knowledge, there is no FE model of the equine MCP. Collins et al. [13] created a FE model of the equine digits which did include the MCP. However, the model was only used to investigate stress within the hoof capsule and the flexor tendons. In addition and perhaps more importantly, the model was not validated. The process of validation is extremely important. It involves comparing the results from the model to known data from the literature or experiments. The assumption is then made that if the model is valid for those parameters that can be measured, then the results obtained for parameters that cannot be experimentally measured are reasonably accurate. Without validation, it is not possible to have confidence in the results of the analysis.

While the overall incidence of catastrophic failure in racehorses during racing and training is low, 0.44 to 1 per 1000 starts [5,15-17], they are catastrophic meaning that they usually result in euthanasia or death of the racehorse. While some of these fractures could be mechanically fixed, biologic complications particularly support limb laminitis many times leads to the ultimate demise of the horse. For this reason, prevention of

injury is especially important. The objective of this study was to create a validated three-dimensional finite element model of the equine metacarpophalangeal joint that can be used to study the risk factors associated with injury and fracture in the hope of developing preventative measures.

## MATERIALS AND METHODS

### *Image acquisition and segmentation*

A computed tomography (CT) scan of the right equine metacarpophalangeal joint (MCP) from mid-MC III to mid-proximal phalanx of a 4 year old gelding weighing 443 kg was obtained from a project unrelated to this study. The scan was performed with a PQCT scanner (Universal Medical Systems, Bedford Hills, NY) at 130 kV and 150 mA with a 1 mm slice thickness in the transverse orientation. The horse had no known history of musculoskeletal disease. Because the CT scan encompassed just the area directly around the MCP and a larger portion of MC III and the proximal phalanx were desired in order to include the origin and attachments of important ligamentous structures, a CT scan of the entire forelimb from a previous project was obtained. The scan was performed with the same CT scanner at 130 kV, 175 mA, and a 4 mm slice thickness for MC III and a 1.5 mm slice thickness for the proximal phalanx. The full forelimb scan was not used for the entire model as the resolution was not sufficient in the area of the MCP.

### *Mesh generation*

The MC III and proximal phalanx from the full forelimb scan was aligned with the respective bones of the MCP scan. The third metacarpal bone, the medial and lateral proximal sesamoid bones (PSB), and the proximal phalanx (PI) as well as the intersesamoidean ligament were manually segmented from the CT images using a commercial software program (Amira, Mercury Computer Systems, Chelmsford, MA).

The segmented geometry was imported into a mesh generation software package (TrueGrid, XYZ Scientific Applications, Livermore, CA) which was used to generate the mesh using hexahedral elements. These elements were chosen because they reduce the computational time by allowing for a reduced mesh density without compromising computational accuracy, especially in comparison to tetrahedral elements, which do not provide accurate predictions when significant bending stress/strains are imposed on the model. The meshed surfaces (bones and intersesamoidean ligament) were then imported into a finite element analysis software package (Abaqus, Simulia, Providence, RI) for analysis. The ligaments (except the intersesamoidean ligament) were defined in Abaqus as non-linear springs (Table 3.1). Elements were extruded at a uniform thickness (0.85 mm, unpublished data) from the bone to represent the articular cartilage. The calcified, middle, and tangential cartilage layers were represented. The middle layer represented the middle and deep layers of the articular cartilage.

### *Material properties*

The bone material properties were determined by mapping the CT density data onto the mesh using custom written code [18]. Well-known relationships between

Hounsfield intensity values and orthotropic elastic moduli have been established for the metaphysis of MC III [19] and the subchondral bone in the distal condyles of MC III [20]. These relationships were used for all of the bones in the MCP.

**Table 3.1:** List of the structures included in the finite element model of the MCP.

<b>Solid Meshed Structures</b>	<b>Non-Linear Springs</b>
Third metacarpal bone	Main, medial and lateral branches of the suspensory ligament
Medial and lateral proximal sesamoid bones	Medial and lateral collateral ligaments
Proximal phalanx	Medial and lateral collateral sesamoidean ligaments
Intersesamoidean ligament	Medial and lateral oblique sesamoidean ligaments
	Straight sesamoidean ligament

The multiphasic nature of articular cartilage is essential to its function [21]. The biphasic poroviscoelastic formulation which allows cartilage to be characterized by a solid phase representing the tissue matrix and a fluid phase representing the synovial fluid has been well-accepted to approximate its compressive mechanical behavior [22]. However in this current study, the equilibrium state as opposed to the dynamic or instantaneous state was of the most interest. Therefore, the modeling of the middle and tangential layers of cartilage was simplified to hyperelastic which still allows for a non-linear response to increasing load. The middle and tangential cartilage layers were defined as hyperelastic using a Mooney-Rivlin model. The hyperelastic coefficients were calculated [23] using a Poisson's ratio of 0.1 [24] and an elastic modulus of 17.9 MPa [25]. The calcified cartilage was defined as an elastic material with a Poisson's ratio of 0.3 and an elastic modulus of 1500. This was done to represent the transition between articular cartilage and the subchondral bone. It is important to represent this transition in

order to decrease potential artifacts due to the sharp change in material properties especially at the osteochondral interface [18,26].

The ligaments were defined as non-linear springs using the stress-strain data from the study by Swanstrom et al. [2]. The suspensory ligament data was used to define the properties for the suspensory ligament and branches. The collateral ligament data was used for the collateral and collateral sesamoidean ligaments. The straight sesamoidean ligament data was used for the straight and oblique sesamoidean ligaments. The data was then adjusted in order to account for the absence of the superficial and deep digital flexor tendons which are important supporting structures.

#### *Boundary conditions and loading*

The center of the coordinate system was defined to be at the center of rotation of the MCP. Positive x was directed medially, positive y was directed dorsally, and positive z was directed distally along MC III. Surface contact between MC III and the proximal phalanx and the proximal sesamoid bones was defined as finite frictionless sliding. The proximal phalanx was initially constrained in only displacement and a concentrated load of 5 N, 5 N, and 50 N in the x, y, and z directions respectively was applied to the proximal aspect of MC III. This was done to allow for settling of the bones. The proximal phalanx was then constrained to allow only rotation around the x-axis. A concentrated load of 120 N, 385 N, and 4568 N in the x, y, and z direction respectively was then applied to the proximal aspect of MC III. These loads were based on the gallop load found during the *in vitro* experiments (Chapter 2)

### *Convergence*

Converging the model is an important step in the development of FE models in order to ensure that accurate predictions are being made in the minimum amount of computational time. In order to perform convergence, models with different mesh resolutions are created for convergence studies. The lower resolution models are compared to the highest resolution model. If the difference between a lower resolution model and the highest resolution model is within the convergence criterion, that model is said to be converged. If none of the lower resolution models fall within the convergence criterion, the process is repeated. The highest resolution model becomes the lowest resolution model and additional models are created with greater mesh density. For the purposes of this study, three initial models of varying mesh density labeled as low, medium, and high were created. Strain energy density of the different bony and soft tissue structures from the low and medium resolution meshes was compared to the high resolution mesh [27]. Convergence criterion was defined as a  $\pm 5\%$  difference from the high resolution mesh.

### *Validation*

Validation is a crucial part in the development of any computer model in order to have confidence in its predictions. The converged FE model was validated using data from the literature as well as a series of cadaveric experiments (described in Chapter 2). Surface contact pressure, bone strain, and ligament strain data were compared to the predictions from the FE model using boundary and loading conditions from the *in vitro* experiments.

## RESULTS

A model of the equine metacarpophalangeal joint was successfully created based on CT image data (Figure 3.1). The model included five structures (four bones and the intersesamoidean ligament) meshed with hexahedral elements and ten ligaments represented with non-linear springs (Table 3.1).

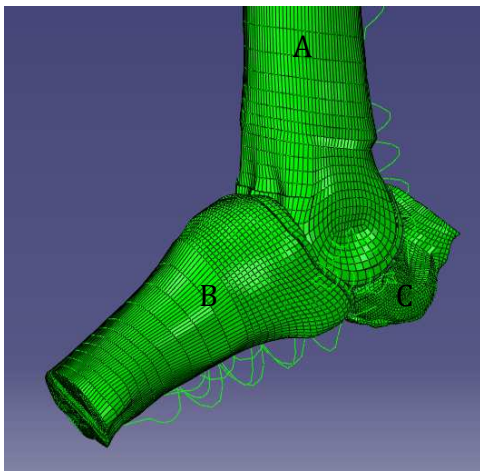


**Figure 3.1:** Medial view of finite element model of the equine MCP at the gallop load. A: MC III, B: proximal phalanx, C: medial proximal sesamoid bone and intersesamoidean ligament.

### *Convergence*

Three models ranging from 78,148 to 158,756 elements were created (Table 3.2). Table 3.3 shows the results from the comparison of the strain energy density between the lower resolution models and the highest resolution model. Convergence within  $\pm 5\%$  was obtained for the medium resolution model.

**Table 3.2:** Convergence parameters for the three models.

<b>Resolution</b>	<b># of Nodes</b>	<b># of Elements</b>	<b>Degrees of Freedom</b>
Low	85181	78148	285993
Med	121533	112633	404709
High	169749	158756	555969

**Table 3.3:** Percent difference in strain energy density of the bony and soft tissue structures between the selected model and the high resolution model averaged over the walk, trot, and gallop loads.

<b>Resolution</b>	<b>MC III</b>	<b>PI</b>	<b>Lat PSB</b>	<b>Med PSB</b>	<b>MC III Cart</b>	<b>PI Cart</b>	<b>PSB Cart</b>
<u>(Low - High)</u> High	-4.26%	-4.20%	-4.49%	-0.84%	-0.78%	-8.90%	0.13%
<u>(Med - High)</u> High	0.97%	-1.21%	4.12%	3.08%	1.15%	-3.81%	0.74%

Lat: lateral, Med: medial, Cart: cartilage

### *Validation*

The medium resolution model was within the convergence criterion for all structures. Based on the convergence results, the medium resolution model was chosen and used for validation purposes. Figure 3.2 shows the comparison of the surface contact pressure values. The model tends to underestimate the pressure at the walk and trot loads. However at the gallop load, model and experimental values are in good agreement. The values reported for Brama et al. [28] include the whole articulating surface of PI as opposed to being broken down between the medial and lateral aspects.

A comparison of the pressure distribution pattern on MC III due to contact with the proximal sesamoid bones found during *in vitro* experiments and from the FE analysis is shown in Figure 3.3. There is good agreement between the model, *in vitro* experimental values, and data from the literature for maximum principal bone strain (Figure 3.4) and ligament strain (Figure 3.5) as well.

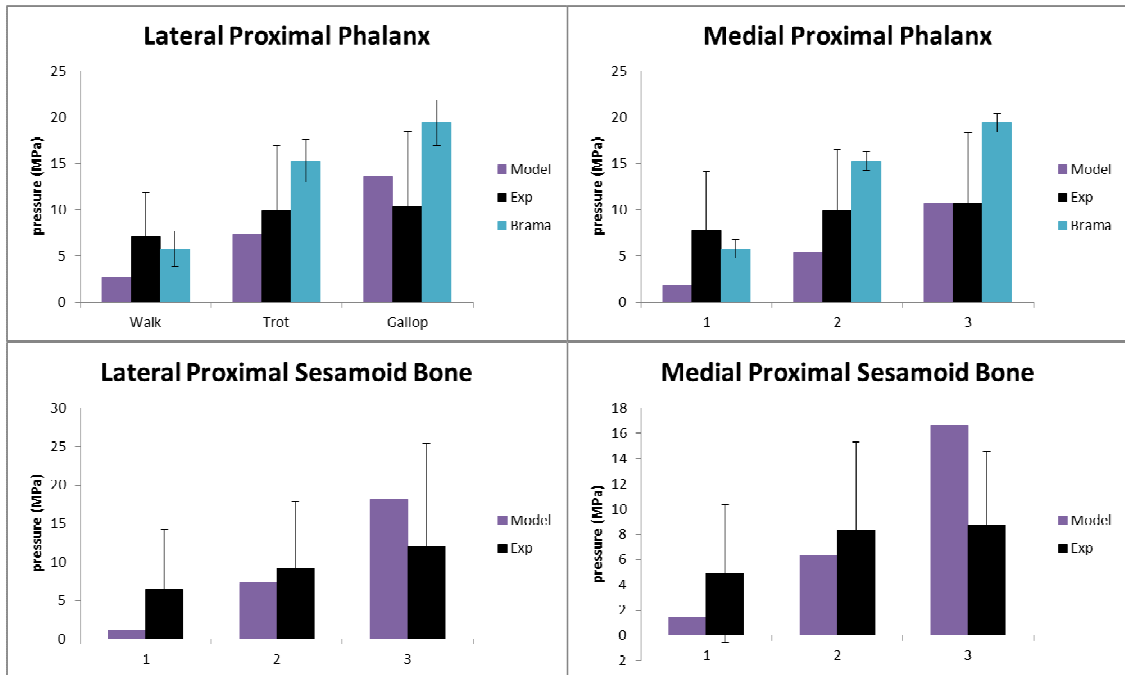


**Figure 3.2:** Comparison of surface contact pressure values (mean  $\pm$  stddev) between the model, *in vitro* experiments, and literature [28]. Values from the literature are for the whole articulating surface of PI as opposed to being broken down between the medial and lateral aspects.

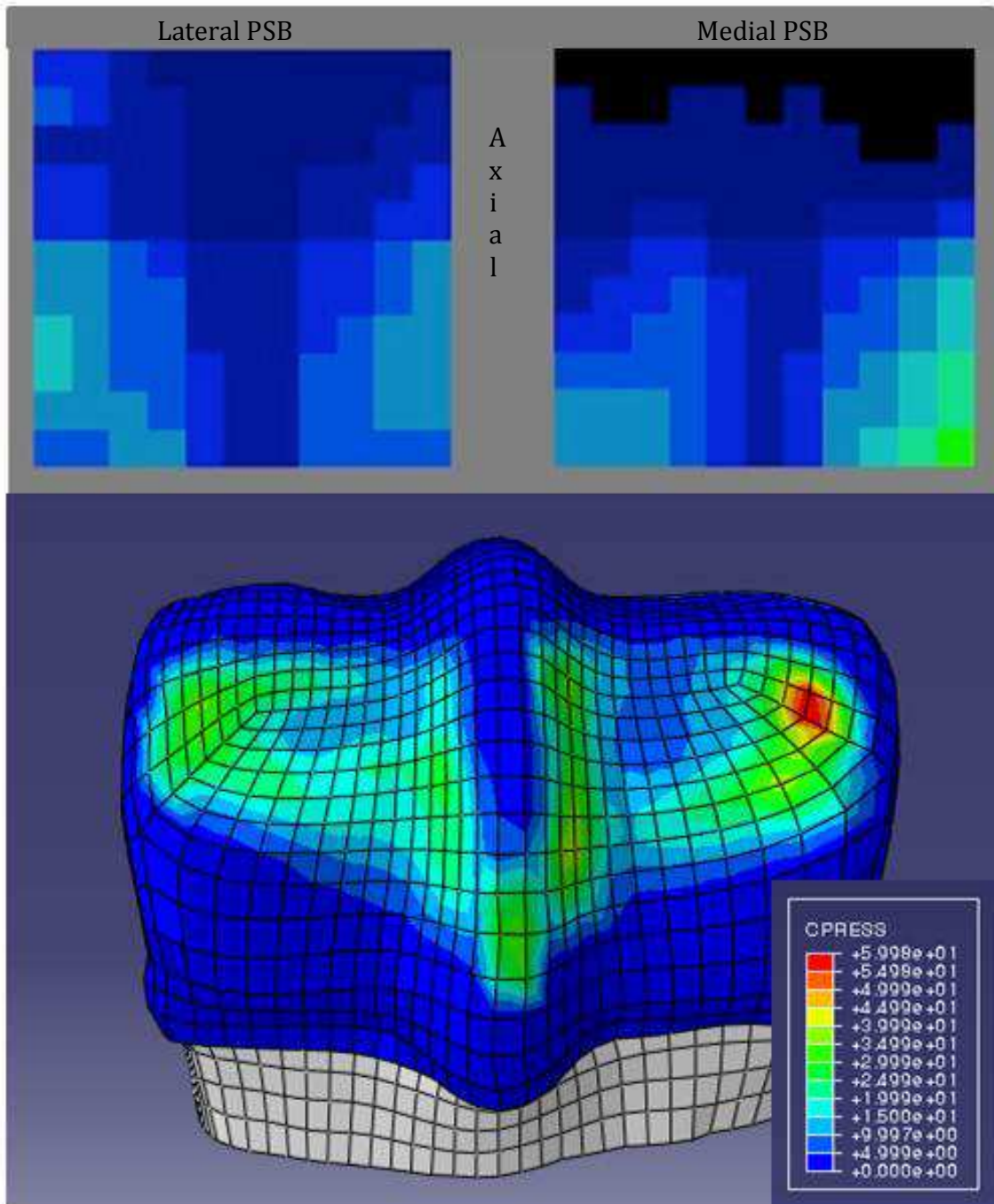


**Figure 3.3:** Pressure distribution pattern on MC III due to contact with the proximal sesamoid bones at the gallop load from *in vitro* experiments (top) and FE model (bottom).

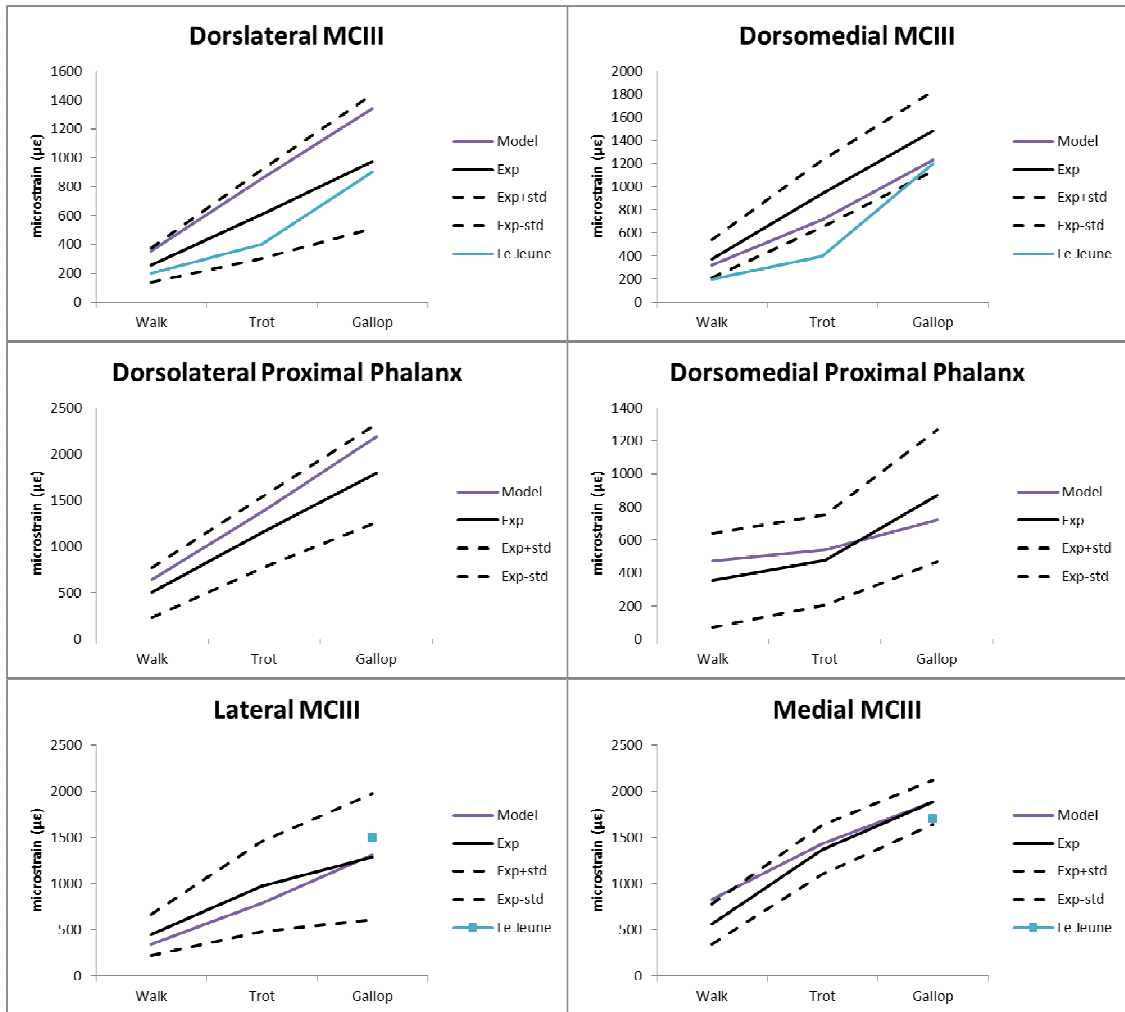


**Figure 3.4:** Comparison of maximum compressive bone strain at various locations at walk, trot, and gallop loads between the model, *in vitro* experiments, and literature [1]. Dashed lines represent  $\pm 1$  stdev of the experimental values.

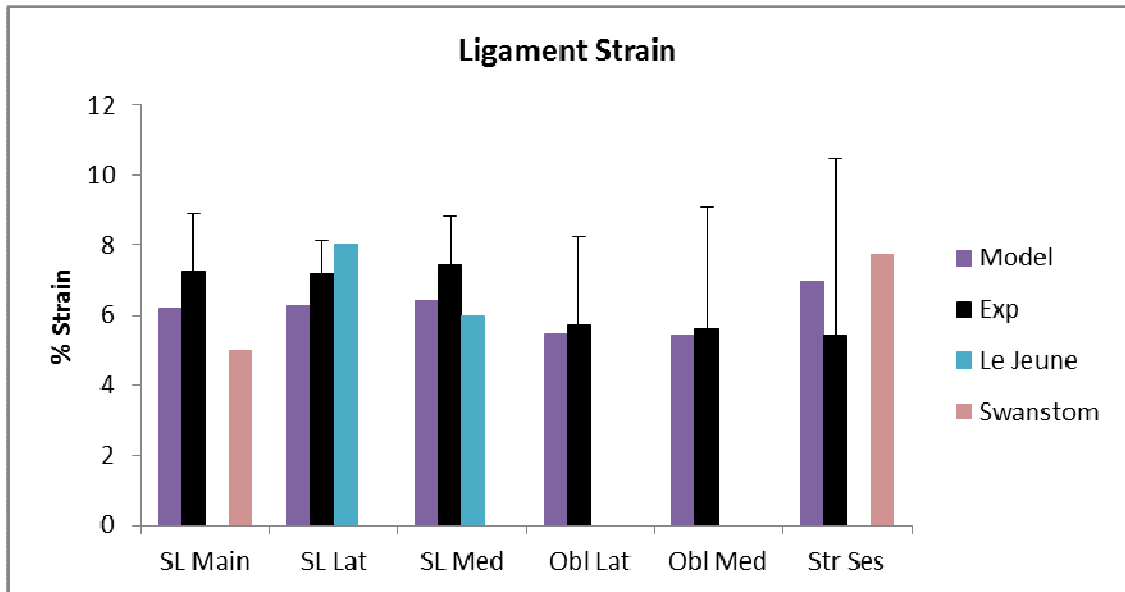


**Figure 3.5:** Comparison of ligament strain between the model, *in vitro* experiments, and the literature [1,2]. Standard deviation reported where available.

## DISCUSSION

A converged, validated model of the equine metacarpophalangeal joint was successfully created. The model contained 121,533 nodes, 112,633 hexahedral elements, and 10 non-linear springs. Validation is an essential part of the creation of a finite element model. The model created in this study was validated based on surface contact pressure, bone strain, and ligament strain data.

There was good agreement between the model and experimental data for the contact pressure especially at the gallop load. The standard deviations for the experimental data were large due to the difficulty in inserting the sensors into the joint and problems with the sensor being pinched as it exited the joint. In addition, each of the four sensing areas only covered a 14 x 14 mm area. These issues could lead to differences between the model and experimental values especially at the walk and trot

loads where part of the sensor was not in the area of contact. At the gallop load where the sensors were in the major area of contact, the values compared well. There is very little data on pressure distribution in the equine MCP joint in the literature. Brama et al. (2001) used pressure sensitive film to investigate pressure distribution and magnitude of the proximal phalanx. The values obtained were much higher than that found in this study. However in the study by Brama et al., the entire articular surface of the proximal phalanx was covered with pressure sensitive film whereas in the current study the sensors were placed on the dorsal aspect of the distal condyles of MC III where PI would articulate. The sensors only covered a 14 x 14 mm area on the medial and lateral condyle. Brama et al. found that the highest pressure was located at the dorsal articular margin of the proximal phalanx. Although the sensors were placed as dorsally as possible on MC III, it is possible that they did not cover this area of highest pressure.

To the author's knowledge, no other study has looked at the pressure distribution due to the proximal sesamoid bones. Similar to the proximal phalanx, values compared well to the experimental data especially at the gallop load. In addition as seen in Figure 3.3, the pattern between experimental data and the FE analysis was very similar. Both showed higher pressures in the axial and abaxial regions and relatively low pressure in the parasagittal groove and central condyle area.

The majority of the equine MCP bone strain data in the literature is for the mid-diaphysis of MC III. One study [1] did investigate strain at the dorsal midpoints of the medial and lateral MC III condyles just proximal to the articular cartilage as well as at the medial and lateral edges of MC III just proximal to the origin of the short fibers of the

collateral ligaments. The model was in good agreement with both this study and the experimental data.

In order to reduce the complexity of the model, the superficial and deep digital flexor tendons were omitted from the model. Both of the flexor tendons represent important support structures of the MCP. The material properties of the suspensory ligament and the distal sesamoidean ligaments were adjusted in order to compensate for the lack of these support structures. Ideally, the flexor tendons would have been included in the model. A CT and MRI of the forelimb in stance position would be necessary to obtain accurate starting positions of the soft tissue structures in order for this to be possible. However as seen in Figure 3.5, the strain values for the suspensory ligament and distal sesamoidean ligaments obtained from the model compare well to the experimental data and that found in the literature suggesting that the adjustment in material properties compensated adequately for the lack of the flexor tendon support.

While simplifying assumptions have been made in the creation of the finite element model of the equine MCP, model results compared well to experimental and published data. Future studies can use this model to study such things as the effect of material properties and bony geometry on stress distribution patterns within the joint. In addition, the model can be further developed to include the flexor tendons and investigate their role in the incidence of injury.

## REFERENCES

- [1] Le Jeune SS, Macdonald MH, Stover SM, Taylor KT, Gerdes M. Biomechanical investigation of the association between suspensory ligament injury and lateral condylar fracture in thoroughbred racehorses. *Vet Surg* 2003;32:585-597.
- [2] Swanstrom MD, Zarucco L, Hubbard M, Stover SM, Hawkins DA. Musculoskeletal modeling and dynamic simulation of the thoroughbred equine forelimb during stance phase of the gallop. *J Biomech Eng* 2005;127:318-328.
- [3] Parkin TD, Clegg PD, French NP, Proudman CJ, Riggs CM, Singer ER, Webbon PM, Morgan KL. Risk of fatal distal limb fractures among Thoroughbreds involved in the five types of racing in the United Kingdom. *Vet Rec* 2004;154:493-497.
- [4] Johnson BJ, Stover SM, Daft BM, Kinde H, Read DH, Barr BC, Anderson M, Moore J, Woods L, Stoltz J, et al. Causes of death in racehorses over a 2 year period. *Equine Vet J* 1994;26:327-330.
- [5] Estberg L, Stover SM, Gardner IA, Johnson BJ, Case JT, Ardans A, Read DH, Anderson ML, Barr BC, Daft BM, Kinde H, Moore J, Stoltz J, Woods LW. Fatal musculoskeletal injuries incurred during racing and training in Thoroughbreds. *J Am Vet Med Assoc* 1996;208:92-96.
- [6] Niebur GL, Feldstein MJ, Yuen JC, Chen TJ, Keaveny TM. High-resolution finite element models with tissue strength asymmetry accurately predict failure of trabecular bone. *J Biomech* 2000;33:1575-1583.
- [7] Keyak JH, Rossi SA, Jones KA, Les CM, Skinner HB. Prediction of fracture location in the proximal femur using finite element models. *Med Eng Phys* 2001;23:657-664.
- [8] Van Rietbergen B, Muller R, Ulrich D, Ruegsegger P, Huiskes R. Tissue stresses and strain in trabeculae of a canine proximal femur can be quantified from computer reconstructions. *J Biomech* 1999;32:443-451.
- [9] Anderson DD, Goldsworthy JK, Li W, James Rudert M, Tochigi Y, Brown TD. Physical validation of a patient-specific contact finite element model of the ankle. *J Biomech* 2007;40:1662-1669.
- [10] Les CM, Keyak JH, Stover SM, Taylor KT. Development and validation of a series of three-dimensional finite element models of the equine metacarpus. *J Biomech* 1997;30:737-742.
- [11] Wullschleger L, Weisse B, Blaser D, Furst AE. Parameter study for the finite element modelling of long bones with computed-tomography-imaging-based stiffness distribution. *Proc Inst Mech Eng H* 2010;224:1095-1107.

- [12] Bowker RM, Atkinson PJ, Atkinson TS, Haut RC. Effect of contact stress in bones of the distal interphalangeal joint on microscopic changes in articular cartilage and ligaments. *Am J Vet Res* 2001;62:414-424.
- [13] Collins SN, Murray RC, Kneissl S, Stanek C, Hinterhofer C. Thirty-two component finite element models of a horse and donkey digit. *Equine Vet J* 2009;41:219-224.
- [14] Thomason JJ, McClinchey HL, Faramarzi B, Jofriet JC. Mechanical behavior and quantitative morphology of the equine laminar junction. *Anat Rec A Discov Mol Cell Evol Biol* 2005;283:366-379.
- [15] Boden LA, Anderson GA, Charles JA, Morgan KL, Morton JM, Parkin TD, Slocombe RF, Clarke AF. Risk of fatality and causes of death of Thoroughbred horses associated with racing in Victoria, Australia: 1989-2004. *Equine Vet J* 2006;38:312-318.
- [16] McKee SL. An update on racing fatalities in the UK. *Equine Vet Educ* 1995;7:202-204.
- [17] Peloso JG, Mundy GD, Cohen ND. Prevalence of, and factors associated with, musculoskeletal racing injuries of Thoroughbreds. *J Am Vet Med Assoc* 1994;204:620-626.
- [18] Womack W. Computational modeling of the lower cervical spine: facet cartilage distribution and disc replacement. *Mechanical Engineering*. Fort Collins: Colorado State University, 2009.
- [19] Les CM, Keyak JH, Stover SM, Taylor KT, Kaneps AJ. Estimation of material properties in the equine metacarpus with use of quantitative computed tomography. *J Orthop Res* 1994;12:822-833.
- [20] Leahy PD, Smith BS, Easton KL, Kawcak CE, Eickhoff JC, Shetye SS, Puttlitz CM. Correlation of mechanical properties within the equine third metacarpal with trabecular bending and multi-density micro-computed tomography data. *Bone* 2010;46:1108-1113.
- [21] Ateshian GA, Mow VC. Friction, lubrication, and wear of articular cartilage and diarthrodial joints In: Mow VC, Huijskes R, eds. *Basic orthopaedic biomechanics and mechano-biology*. 3 ed. Philadelphia: Lippincott Williams and Wilkins, 2005;447-494.
- [22] Mow VC, Gu WY, Chen FH. Structure and function of articular cartilage and meniscus In: Mow VC, Huijskes R, eds. *Basic orthopaedic biomechanics and mechano-biology*. 3 ed. Philadelphia: Lippincott Williams and Wilkins, 2005;181-258.
- [23] Bower AF. *Applied Mechanics of Solids*. Boca Raton: CRC Press, 2009.

- [24] Palmer JL, Bertone AL, Malesud CJ, Mansour J. Biochemical and biomechanical alterations in equine articular cartilage following an experimentally-induced synovitis. *Osteoarthritis Cartilage* 1996;4:127-137.
- [25] Lewis CW, Williamson AK, Chen AC, Bae WC, Temple MM, Van Wong W, Nugent GE, James SP, Wheeler DL, Sah RL, Kawcak CE. Evaluation of subchondral bone mineral density associated with articular cartilage structure and integrity in healthy equine joints with different functional demands. *Am J Vet Res* 2005;66:1823-1829.
- [26] Mente PL, Lewis JL. Elastic modulus of calcified cartilage is an order of magnitude less than that of subchondral bone. *J Orthop Res* 1994;12:637-647.
- [27] Ayturk UM, Puttlitz CM. The effect of mesh refinement on the predictions of finite element models of spine. ASME Summer Bioengineering Conference 2009.
- [28] Brama PA, Karssenber D, Barneveld A, van Weeren PR. Contact areas and pressure distribution on the proximal articular surface of the proximal phalanx under sagittal plane loading. *Equine Vet J* 2001;33:26-32.

CHAPTER 4  
EFFECT OF BONE GEOMETRY ON CONTACT STRESS IN THE EQUINE  
METACARPOPHALANGEAL JOINT

INTRODUCTION

The metacarpophalangeal joint (MCP) is one of the most commonly injured joints in Thoroughbred racehorses. The lateral condyle of the third metacarpal bone (MC III) and the proximal sesamoid bones are the most frequently fractured [1-5]. These injuries are generally career ending and many times life ending as well. Prevention is key due to the catastrophic nature of these injuries as well as their associated complications making treatment difficult at best. Therefore, determination of factors that can identify horses at risk for failure is essential for the wellbeing of the racehorse and the sport itself.

Previous studies have shown that conformation and joint geometry are risk factors for musculoskeletal injury in the Thoroughbred racehorse. Offset knees and an increase in front pastern length [7], hoof shape and balance [8], and the ratio of lateral to medial condylar width and the radius of curvature of the distal condyles of MC III [9] have all been shown to be indicators of increased risk of injury.

As injuries to the MCP account for the majority of the career ending and catastrophic injuries in Thoroughbred racehorses, the objective of this study was to determine how geometric variations in the MCP may predispose a horse to injury. In

order to accomplish this, a converged, validated finite element (FE) model of the equine MCP (Chapter 3) was morphed to create 3 FE models of the MCP from three different horses: one that had suffered a catastrophic fracture of the lateral condyle, one from the contralateral limb of a horse that had suffered a catastrophic fracture of the lateral condyle, and one from a control horse. Specifically, it was hypothesized that there would be differences in the stress distribution pattern between the three groups that could help further elucidate the pathogenesis of fracture in the equine MCP.

## MATERIALS AND METHODS

### *Selection of bone geometry data*

Computed tomography (CT) data for three MCP joints from three different horses were selected from a dataset of 100 horses: 50 control and 50 that had suffered from a condylar fracture. The dataset was split into three groups: control, fractured, and non-fractured (limb contralateral to the fractured limb). Previous studies have shown significant differences in the ratio of the lateral and medial condylar width as well as the radius of curvature between the three groups [9]. Selection of the joints was based on determining the joint that best represented the average condylar width ratio and radius of curvature measurements of each respective group. For the fracture group, due to the disruption of the bony geometry caused by the fracture, the joint in the non-fractured group that best represented the fractured group was chosen.

### *Morphing the model*

The converged, validated model developed as described in Chapter 3 was morphed based on the CT data to create three finite element (FE) models. Surface reconstructions of the bones from the CT data were created using a commercial software program (Amira 4.1.1, Mercury Computer Systems, Chelmsford, MA). The base FE model was imported into the program and was morphed using the Landmark Surface Warp function [10]. The morphed mesh was compared to the surface reconstruction in order to ensure an accurate geometric representation of the joint surface.

### *Boundary conditions and loading*

The morphed models were imported into a FE analysis program (Abaqus 6.9, Simulia, Providence, RI) for analysis. Boundary conditions and loading were as described in Chapter 3. Briefly, the coordinate system was defined with the center at the center of rotation of the MCP, positive x directed medially, positive y directed dorsally, and positive z directed distally. The proximal phalanx was constrained to allow only rotation around the x-axis. A concentrated load of 120 N, 385 N, and 4568 N was applied in the x, y, and z directions respectively. This load was chosen to simulate the stance phase of gallop as found during the *in vitro* experiments (Chapter 2).

### *Analysis*

The von Mises stress was subjectively compared between the control, fractured, and contralateral MCP models for the cartilage and bone of the distal condyles of MC III. In addition, the average von Mises stress for the medial and lateral parasagittal grooves at

30° palmar to the transverse ridge was compared between the three condyles. This area was chosen as fractures of the lateral condyle are thought to initiate in this location.

## RESULTS

Three finite element models were successfully created by morphing the base model created in Chapter 3. There was good agreement between the morphed model and the actual geometry especially in the areas of contact (Figure 4.1).

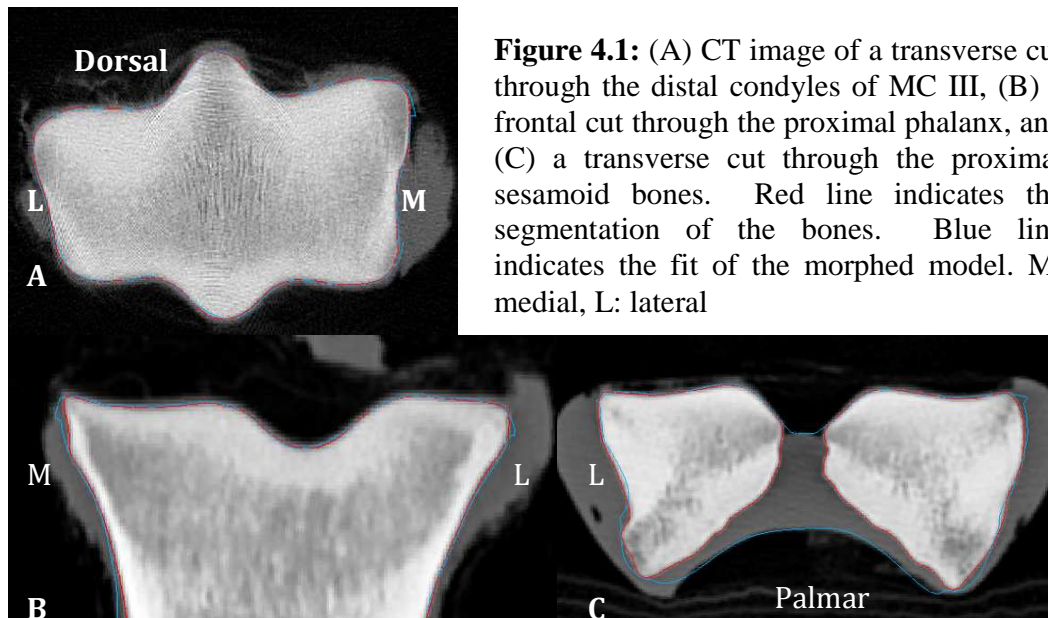
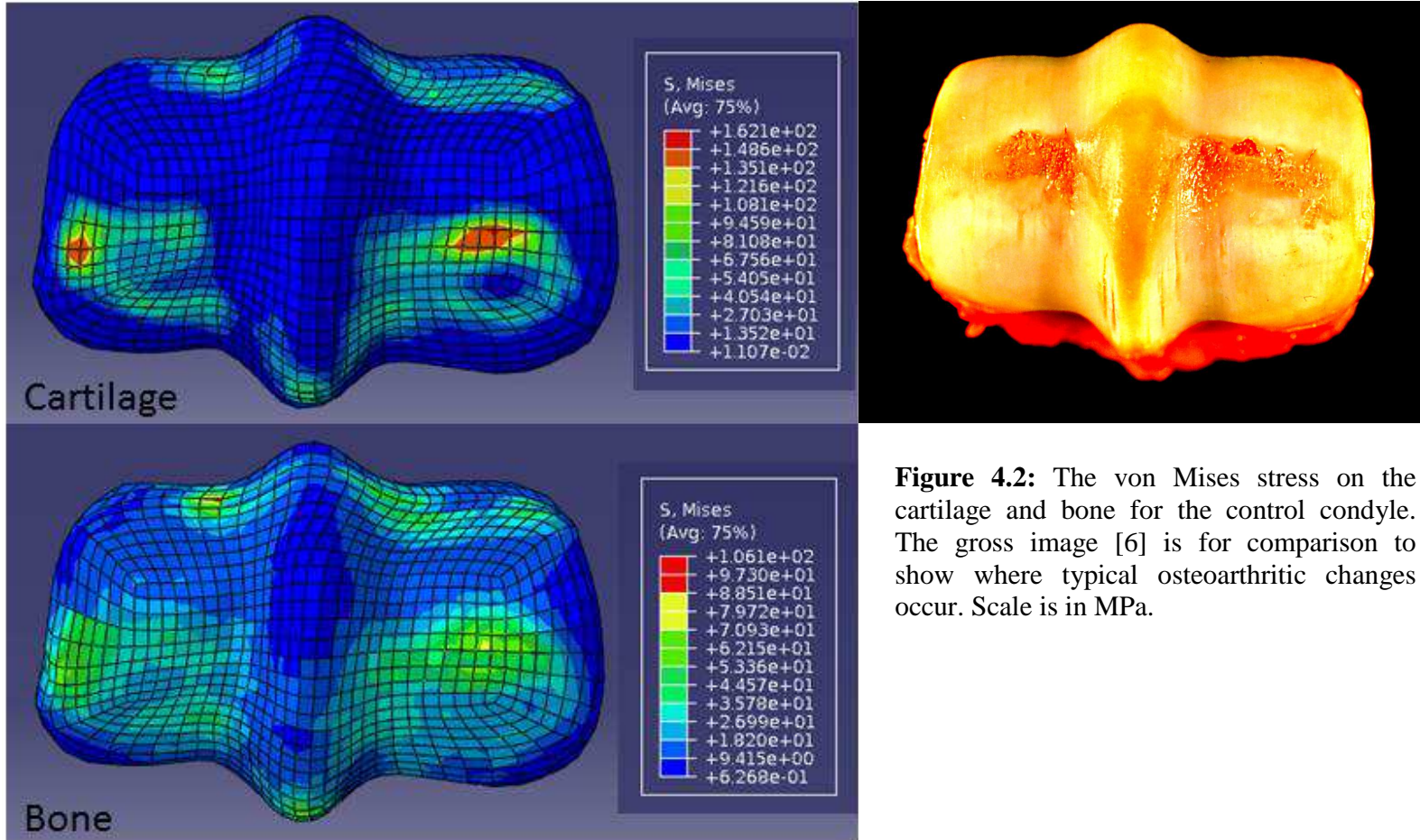


Figure 4.2 shows the von Mises stress for the cartilage and bone for the control condyle. The figure shows an area of high stress on the cartilage in the area of the transverse ridge. The gross picture (Figure 4.2) is of a condyle that depicts the osteoarthritic changes that can be seen. As can be seen, there were severe changes in the area of the transverse ridge where the highest cartilage stresses occurred. While the

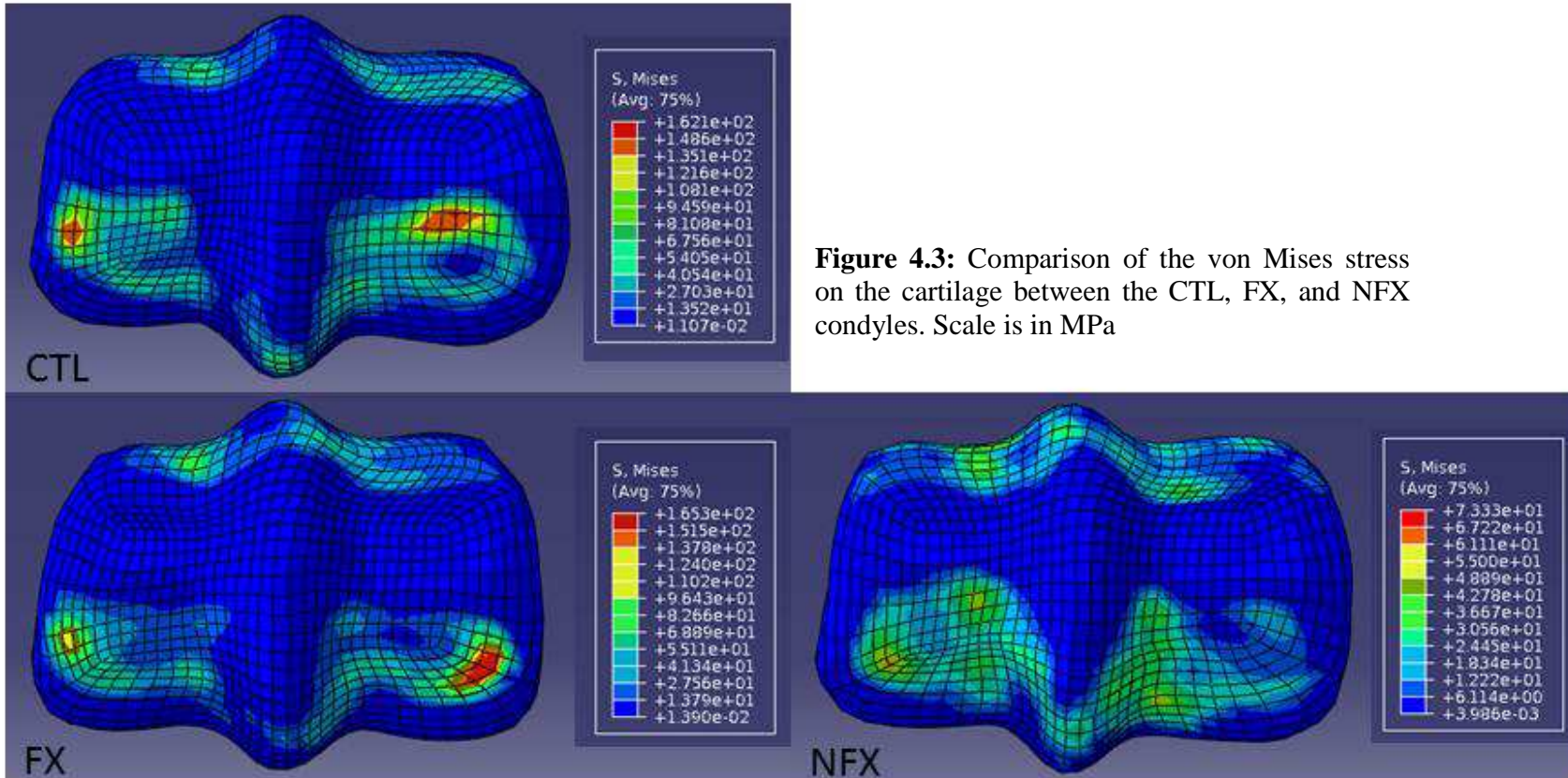
stress was still highest in the area of the transverse ridge on the bone, the stress was spread out over a greater area on the condyles than seen on the cartilage.

Figure 4.3 and Figure 4.4 show the von Mises stress for the control (CTL), fractured (FX), and contralateral nonfractured (NFX) condyles on the cartilage and the bone respectively. As can be appreciated from the figures, there were some noticeable differences in the stress pattern between the three condyles. For the CTL condyle, the area of highest stress in the cartilage occurred in the region of the transverse ridge. In contrast, the highest stresses in the NFX and FX condyles tended towards the region of the parasagittal grooves and 30° palmar region respectively. The bone stresses were more diffuse over the condyles in all three condyles. However, they showed distribution patterns similar to those found on the cartilage.

Figure 4.5 shows the von Mises stress for the CTL, FX, and NFX condyles on a 30° palmar slice. In all three condyles, there was an area of increased stress in the region of both the medial and lateral parasagittal grooves. Figure 4.6 compares the average von Mises stress for the medial and lateral parasagittal grooves at the 30° palmar section. The stress was higher in the medial parasagittal groove area than the lateral parasagittal groove area for all three condyles. The highest stress occurred in the medial parasagittal groove of the FX condyle. Figure 4.7 shows how the stress varied across the condyle from lateral to medial at 30° palmar. As can be seen in the figure, the FX condyle had the greatest variation in stress across the condyle. In addition, for all condyles, the areas of highest stress occurred at approximately the midpoints of the medial and lateral condyles while the area of lowest stress occurred between the midsagittal ridge and the lateral parasagittal groove.



**Figure 4.2:** The von Mises stress on the cartilage and bone for the control condyle. The gross image [6] is for comparison to show where typical osteoarthritic changes occur. Scale is in MPa.



**Figure 4.3:** Comparison of the von Mises stress on the cartilage between the CTL, FX, and NFX condyles. Scale is in MPa

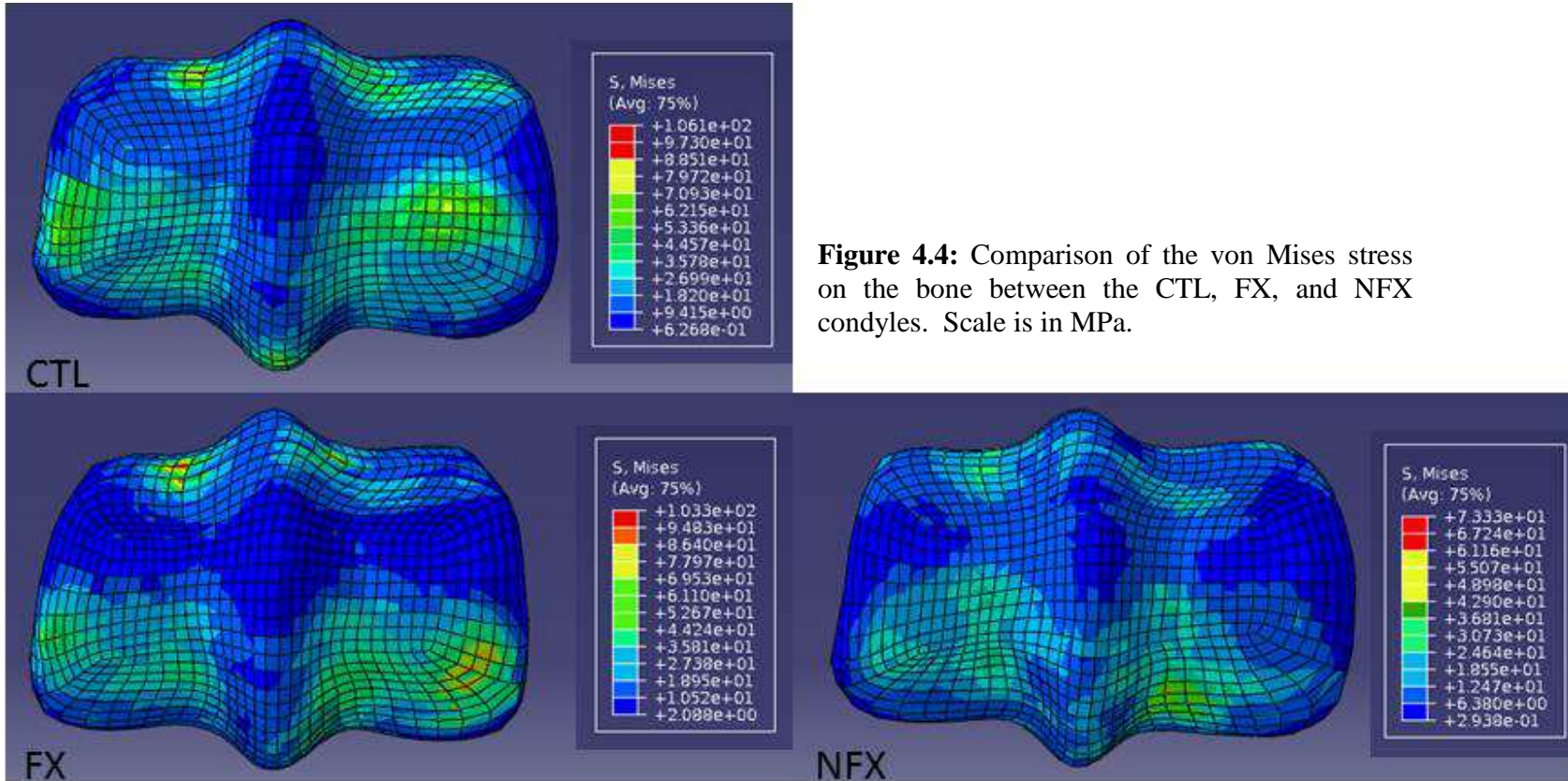


**Figure 4.4:** Comparison of the von Mises stress on the bone between the CTL, FX, and NFX condyles. Scale is in MPa.

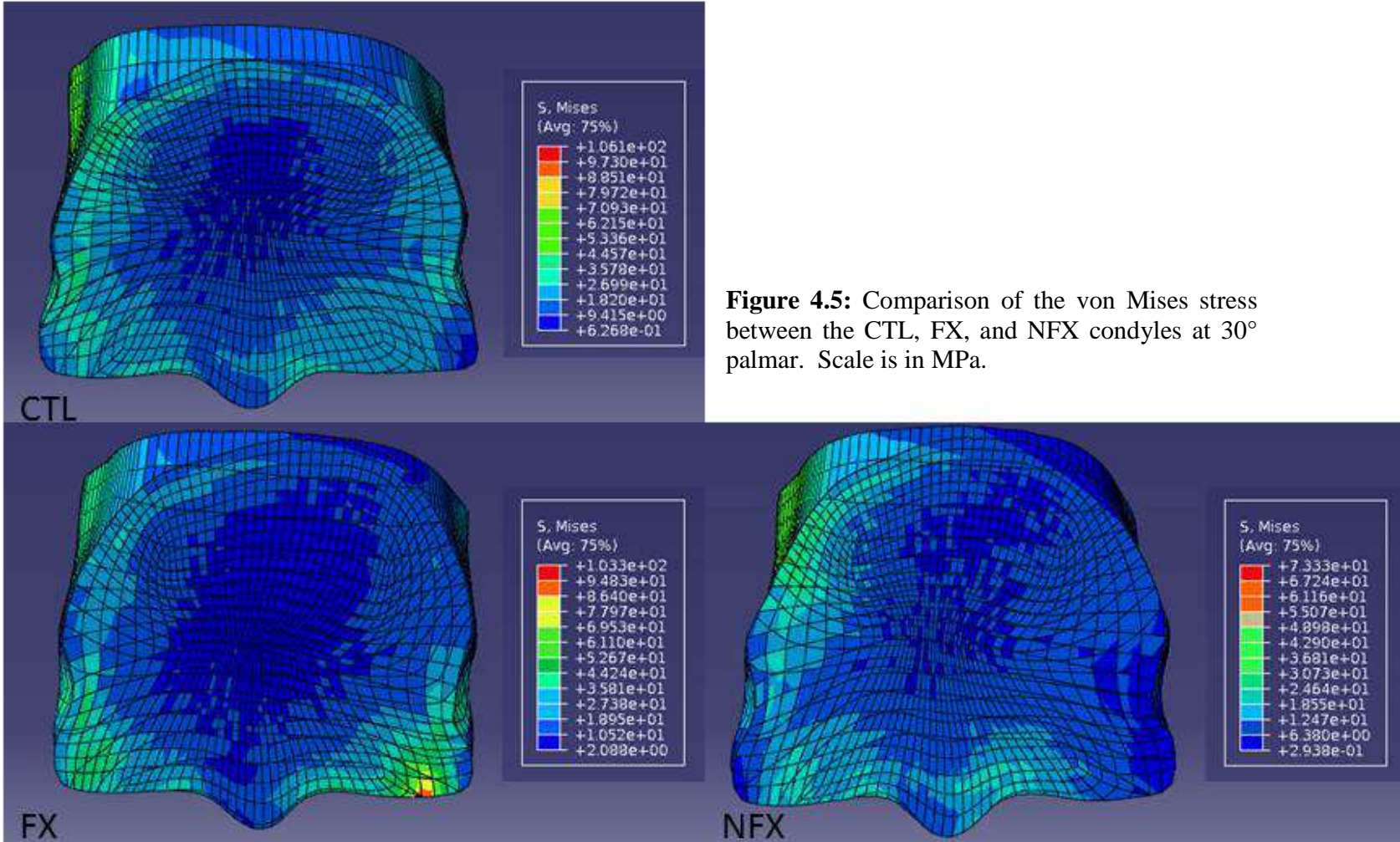


**Figure 4.5:** Comparison of the von Mises stress between the CTL, FX, and NFX condyles at 30° palmar. Scale is in MPa.

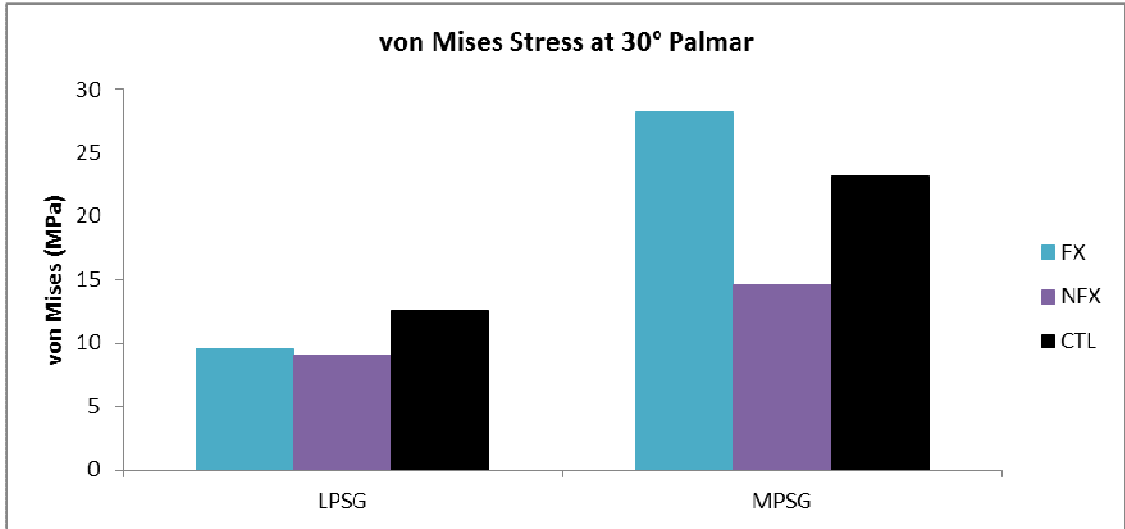


**Figure 4.6:** Graph of the von Mises stress in the lateral (LPSG) and medial (MPSG) parasagittal grooves at 30° palmar for the fracture (FX), non-fracture (NFX) and control (CTL) condyles.

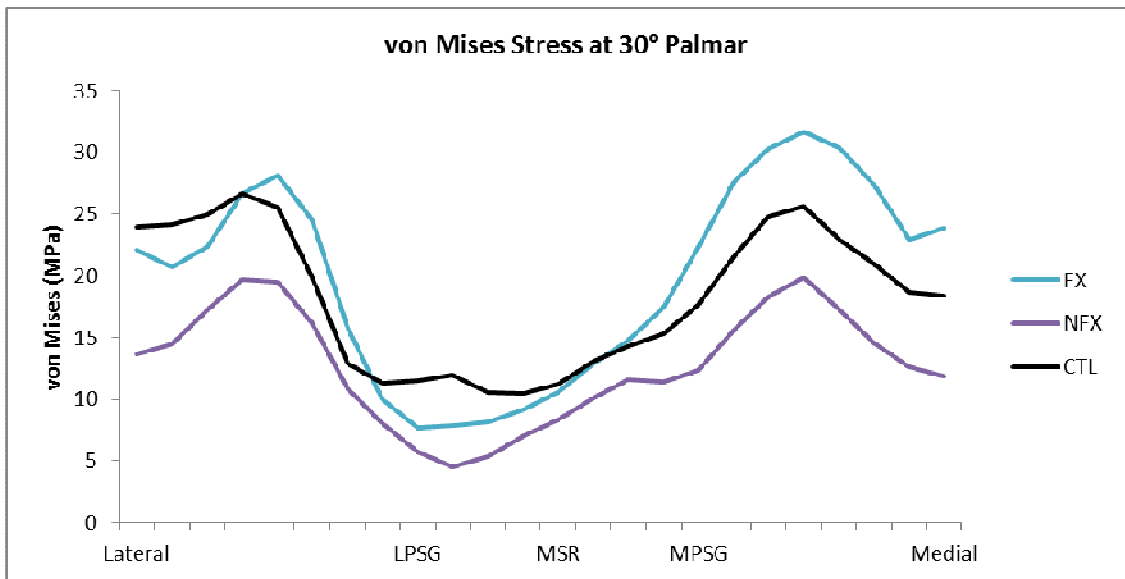


**Figure 4.7:** Graph depicting the von Mises stress along the length of the condyles at 30° palmar for the fracture (FX), non-fracture (NFX) and control (CTL) condyles.

## DISCUSSION

This study used computed tomography data to morph a converged, validated finite element model of the equine metacarpophalangeal joint in order to represent varying geometries found within the joint. It was shown that the landmark based morphing function of a commercially available software package was an effective method of creating additional models based on subject specific image data.

Results from this study supported the hypothesis that there would be differences in the stress distribution pattern due to variations in bone geometry in the equine MCP. The areas of highest stress in both the cartilage and bone tended to occur more palmarly and abaxially in the FX condyle when compared to the CTL and NFX condyle respectively. In the 30° palmar section, increased stress was found in both the medial and lateral parasagittal grooves in all three condyles. Previous studies have shown that fractures of the lateral condyle originated in consistent areas namely the distopalmar aspect of the lateral parasagittal groove. This area was a common site for macroscopic defects in the articular cartilage and underlying subchondral bone. In addition, CT scans revealed radiolucent areas in this area as well [11,12].

Figure 4.5 shows an area of increased stress in the palmar aspect of the lateral and medial parasagittal groove that extends proximally in all three models. This stress distribution pattern can help explain why fractures originating in the palmar aspect of the parasagittal grooves are one of the most common types of catastrophic injury in the equine racehorse.

The medial parasagittal groove area had greater stress in comparison to the lateral parasagittal groove. While lateral condylar fractures are far more common, medial condylar fractures can be seen as well [13,14]. A multitude of other factors could be responsible for the higher incidence of lateral condylar fractures in comparison to medial condylar fractures. These factors could include bone material properties, variations in muscle forces, or side to side differences in ligament laxity. In addition, in investigating the stress pattern along the length of the condyle, it can be seen that there was a gradual increase in stress from the midsagittal ridge medially to mid medial condyle. In contrast, while there is relatively low stress in the lateral parasagittal groove, it was surrounded by two areas of higher stress. It is thought that the relative change in stress may play a larger role than the absolute stress at a given location as long as the absolute stress is less than the yield or ultimate strength. Additional investigations with larger sample sizes are needed in order to further examine this hypothesis.

The yield and ultimate strength of the equine metacarpal condyle in the 30° palmar location has been reported as  $62.69 \pm 19.10$  MPa and  $74.77 \pm 25.14$  MPa respectively [15]. The von Mises stress found in the current study was less than this in all three condyles including the fracture condyle. As discussed above, the stress gradient may play a role in fracture. As can be appreciated in Figure 4.7, the fracture condyle had the largest variation in stress along the length of the condyle. In addition in the control condyle, the stress was relatively constant in the lateral parasagittal groove area. There may be a number of other factors that also play a role. Again, further studies are warranted.

There are a number of limitations to this study. Chronic cyclic loading leading to focal remodeling has been shown to occur in the palmar aspect of the lateral parasagittal groove where fractures are thought to initiate [12]. Therefore, the material properties between the three condyles may in actuality be very different and could contribute significantly to the stress patterns found in the condyle. However, in this study, the material properties were consistent between the three models. Keeping the material properties consistent allowed for a better comparison of the variation in stress patterns due solely to joint geometry. However, the variation in joint geometry undoubtedly affects bone adaptation [16-18] due to differences in how the bones are loaded. In addition, a study by Firth et al. [19] showed differences in mineralization in the area where lateral condylar fractures are thought to initiate before race training had begun. This suggests that some horses may be predisposed to fracture based on initial material properties. In future studies, it would be interesting to define the bony material properties for each model in the FX, NFX, and CTL groups based on the CT data that each respective model is based on.

Likewise, ligament and tendon material properties can vary between individual subjects. Subclinical to mild injuries of the suspensory apparatus have been shown to increase the risk of further musculoskeletal injury [20]. Again, the material properties in the models were held consistent to better study the effect of geometry. However, variations in the soft tissue material properties could lead to changes in how a joint is loaded and consequently the contact stress within a joint [21].

Another possible limitation to this study is the choice of the failure criteria used. The von Mises stress was used in this study to compare the overall stress distribution

pattern between the three models as well as the average stress value in the parasagittal grooves. Some studies have argued that other failure criteria are better. Multiple studies have looked at strain based criteria [22,23], others at stress based criteria [24], and still others at criteria specifically for anisotropic material [25]. Although there is much debate in the literature as to the appropriate failure criteria to use, multiple studies have used von Mises stress to predict fracture location with reasonable accuracy [26,27]. For this reason, the von Mises stress was chosen for this study. In future analyses, it may be beneficial to compare the different criteria as applied to the study of catastrophic injury in racehorses. However, that is beyond the scope of this investigation.

The landmark based morphing method did a good job of morphing the base model providing a relatively efficient method of creating specimen specific models from a converged and validated model. Although the images showed relatively good agreement between the morphed model and the CT scan it was based on, the landmark method does require a certain amount of interpolation between each landmark. Too few landmarks can result in the smoothing over of important geometrical differences. However, too many landmarks can lead to irregularities due to being over-constrained. It would be interesting to look at the effect of the number of landmarks on the model analysis results or compare the landmark based morphed model with a surface based method.

The results presented herein are based on three specimens, one in each group. However, the results based on just these three samples showed that there were some stress distribution patterns in the equine MCP that were similar between the FX, NFX, and CTL condyles and were consistent with areas that are commonly fractured. Other stress distribution patterns were different between the three condyles and could help

better elucidate the pathogenesis of fracture in the racehorse. While it is difficult to draw any definitive conclusions from such a small sample size, this study shows that further studies are warranted. These include increasing the number of models investigated, expanding the model to include the flexor tendons and more distal and proximal structures, and modifying material properties. With further studies, a better understanding of the pathogenesis of catastrophic injuries in Thoroughbred racehorses will be realized which ultimately can lead to our ability to decrease the incidence of these career and sometimes life ending injuries.

## REFERENCES

- [1] Johnson BJ, Stover SM, Daft BM, Kinde H, Read DH, Barr BC, Anderson M, Moore J, Woods L, Stoltz J, et al. Causes of death in racehorses over a 2 year period. *Equine Vet J* 1994;26:327-330.
- [2] Parkin TD, Clegg PD, French NP, Proudman CJ, Riggs CM, Singer ER, Webbon PM, Morgan KL. Risk of fatal distal limb fractures among Thoroughbreds involved in the five types of racing in the United Kingdom. *Vet Rec* 2004;154:493-497.
- [3] Cohen ND, Dresser BT, Peloso JG, Mundy GD, Woods AM. Frequency of musculoskeletal injuries and risk factors associated with injuries incurred in Quarter Horses during races. *J Am Vet Med Assoc* 1999;215:662-669.
- [4] Peloso JG, Mundy GD, Cohen ND. Prevalence of, and factors associated with, musculoskeletal racing injuries of Thoroughbreds. *J Am Vet Med Assoc* 1994;204:620-626.
- [5] Estberg L, Stover SM, Gardner IA, Johnson BJ, Case JT, Ardans A, Read DH, Anderson ML, Barr BC, Daft BM, Kinde H, Moore J, Stoltz J, Woods LW. Fatal musculoskeletal injuries incurred during racing and training in Thoroughbreds. *J Am Vet Med Assoc* 1996;208:92-96.
- [6] McIlwraith CW, Frisbie DD, Kawcak CE, Fuller CJ, Hurtig M, Cruz A. The OARSI histopathology initiative - recommendations for histological assessments of osteoarthritis in the horse. *Osteoarthritis and cartilage / OARS, Osteoarthritis Research Society* 2010;18 Suppl 3:S93-105.
- [7] Anderson TM, McIlwraith CW, Douay P. The role of conformation in musculoskeletal problems in the racing Thoroughbred. *Equine Vet J* 2004;36:571-575.
- [8] Kane AJ, Stover SM, Gardner IA, Bock KB, Case JT, Johnson BJ, Anderson ML, Barr BC, Daft BM, Kinde H, Larochelle D, Moore J, Mysore J, Stoltz J, Woods L, Read DH, Ardans AA. Hoof size, shape, and balance as possible risk factors for catastrophic musculoskeletal injury of Thoroughbred racehorses. *Am J Vet Res* 1998;59:1545-1552.
- [9] Kawcak CE, Zimmerman CA, Easton KL, McIlwraith CW, Parkin TD. Effects of third metacarpal geometry on the incidence of condylar fractures in Thoroughbred racehorses. *Am Assoc of Eq Practitioners* 2009;197.
- [10] Sigal IA, Hardisty MR, Whyne CM. Mesh-morphing algorithms for specimen-specific finite element modeling. *J Biomech* 2008;41:1381-1389.
- [11] Kawcak CE, Bramlage LR, Embertson RM. Diagnosis and management of incomplete fracture of the distal palmar aspect of the third metacarpal bone in five horses. *J Am Vet Med Assoc* 1995;206:335-337.

- [12] Riggs CM, Whitehouse GH, Boyde A. Pathology of the distal condyles of the third metacarpal and third metatarsal bones of the horse. *Equine Vet J* 1999;31:140-148.
- [13] Parkin TD, Clegg PD, French NP, Proudman CJ, Riggs CM, Singer ER, Webbon PM, Morgan KL. Catastrophic fracture of the lateral condyle of the third metacarpus/metatarsus in UK racehorses - fracture descriptions and pre-existing pathology. *Vet J* 2006;171:157-165.
- [14] Zekas LJ, Bramlage LR, Embertson RM, Hance SR. Characterisation of the type and location of fractures of the third metacarpal/metatarsal condyles in 135 horses in central Kentucky (1986-1994). *Equine Vet J* 1999;31:304-308.
- [15] Leahy PD, Smith BS, Easton KL, Kawcak CE, Eickhoff JC, Shetye SS, Puttlitz CM. Correlation of mechanical properties within the equine third metacarpal with trabecular bending and multi-density micro-computed tomography data. *Bone* 2010;46:1108-1113.
- [16] Riggs CM. Fractures--a preventable hazard of racing thoroughbreds? *Vet J* 2002;163:19-29.
- [17] Smith RK, Goodship AE. The effect of early training and the adaptation and conditioning of skeletal tissues. *Vet Clin North Am Equine Pract* 2008;24:37-51.
- [18] Firth EC, Delahunt J, Wichtel JW, Birch HL, Goodship AE. Galloping exercise induces regional changes in bone density within the third and radial carpal bones of Thoroughbred horses. *Equine Vet J* 1999;31:111-115.
- [19] Firth EC, Doube M, Boyde A. Changes in mineralised tissue at the site of origin of condylar fracture are present before athletic training in Thoroughbred horses. *N Z Vet J* 2009;57:278-283.
- [20] Hill AE, Stover SM, Gardner IA, Kane AJ, Whitcomb MB, Emerson AG. Risk factors for and outcomes of noncatastrophic suspensory apparatus injury in Thoroughbred racehorses. *J Am Vet Med Assoc* 2001;218:1136-1144.
- [21] Le Jeune SS, Macdonald MH, Stover SM, Taylor KT, Gerdes M. Biomechanical investigation of the association between suspensory ligament injury and lateral condylar fracture in thoroughbred racehorses. *Vet Surg* 2003;32:585-597.
- [22] Schileo E, Taddei F, Cristofolini L, Viceconti M. Subject-specific finite element models implementing a maximum principal strain criterion are able to estimate failure risk and fracture location on human femurs tested in vitro. *Journal of biomechanics* 2008;41:356-367.
- [23] Nalla RK, Kinney JH, Ritchie RO. Mechanistic fracture criteria for the failure of human cortical bone. *Nat Mater* 2003;2:164-168.

- [24] Bessho M, Ohnishi I, Matsuyama J, Matsumoto T, Imai K, Nakamura K. Prediction of strength and strain of the proximal femur by a CT-based finite element method. *Journal of biomechanics* 2007;40:1745-1753.
- [25] Keaveny TM, Wachtel EF, Zadesky SP, Arramon YP. Application of the Tsai-Wu quadratic multiaxial failure criterion to bovine trabecular bone. *Journal of biomechanical engineering* 1999;121:99-107.
- [26] Keyak JH, Rossi SA, Jones KA, Les CM, Skinner HB. Prediction of fracture location in the proximal femur using finite element models. *Med Eng Phys* 2001;23:657-664.
- [27] Yosibash Z, Tal D, Trabelsi N. Predicting the yield of the proximal femur using high-order finite-element analysis with inhomogeneous orthotropic material properties. *Philos Transact A Math Phys Eng Sci* 2010;368:2707-2723.

## SUMMARY AND FUTURE DIRECTIONS

This study has set the framework for future investigations into the stress distribution patterns and possible mechanisms of catastrophic failure within the equine metacarpophalangeal joint using finite element modeling. The *in vitro* portion of this project has provided a robust data set that can be used to validate future finite element models. In addition, between the third metacarpal bone and the proximal sesamoid bones, an area of high pressure axially and abaxially with a relatively low pressure area in the center was found. This type of pressure distribution pattern may lead to undue stress in the area of the parasagittal groove where many condylar fractures are thought to initiate.

The second portion of the study created a converged and validated finite element model of the equine metacarpophalangeal joint. While many other finite element models of various equine bones have been created, none to this point have been used to study the possible mechanisms of catastrophic injury in the metacarpophalangeal joint. The use of finite element models provides a fantastic way of investigating various parameters by allowing the user to change individual parameters such as bone geometry and material properties and then determine what effect if any those properties have on the stress within a joint. This can help direct clinical studies without having to sacrifice a large number of research animals for controlled experimental studies.

The use of the finite element model to study the effect of bone geometry provided insight into the pathogenesis of fracture. Increased stress was found in the parasagittal groove area just palmar to the transverse ridge. This area is where many condylar fractures are thought to initiate. In addition, there were noticeable differences in the stress distribution pattern between the control, fractured, and non-fractured contralateral limb models. Further study of these differences can help lead to a better understanding of the factors that predispose one horse to catastrophic failure while another horse can have a successful racing career.

There are many directions that the research can go from here in order to have a greater understanding of the pathogenesis of catastrophic failure in Thoroughbred racehorses. Additional work on the model to include the flexor tendons as well as more distal and proximal structures will be an important start. Extending the scope of the model may allow for the inclusion of muscle forces. Investigating the role of material properties, both bone and soft tissue, will likely lead to significant differences as well. This study represents just the beginning. With continued work and a better understanding, it is hoped that we can ultimately decrease the incidence of catastrophic injury and improve the welfare of Thoroughbred racehorses.